



Reconstructing Holocene temperature and salinity variations in the western Baltic Sea region: A multi-proxy comparison from the Little Belt (IODP Expedition 347, Site M0059)

Ulrich Kotthoff^{1,2}, Jeroen Groeneveld³, Jeanine L. Ash⁴, Anne-Sophie Fanget⁵, Nadine Quintana Krupinski⁶, Odile Peyron⁷, Anna Stepanova⁸, Jonathan Warnock⁹, Niels A. G. M. Van Helmond¹⁰,
5 Benjamin H. Passey¹¹, Ole Rønø Clausen⁵, Ole Bennike¹², Elinor Andrén¹³, Wojciech Granoszewski¹⁴,
Thomas Andrén¹³, Helena L. Filipsson⁶, Marit-Solveig Seidenkrantz⁵, Caroline P. Slomp¹⁰, Thorsten Bauersachs¹⁵

¹Institute for Geology, University of Hamburg, D-20146, Hamburg, Germany

²Center of Natural History, University of Hamburg, Hamburg, D-20146, Germany

10 ³MARUM, Center for Marine Environmental Sciences, University of Bremen, D-28359, Bremen, Germany

⁴Department of Earth, Planetary, and Space Sciences, UCLA, 90024, USA

⁵Centre for Past Climate Studies, Department of Geoscience, Aarhus University, 8000 Aarhus C, Denmark

15 ⁶Department of Geology, Lund University, 22362 Lund, Sweden

⁷Institut des Sciences de l'Évolution, UMR 5554, Université de Montpellier, 34095 Montpellier cedex 05 France

⁸Department of Computer Science and Engineering, Texas A&M University, 77843, USA

⁹Department of Geoscience, Indiana University of Pennsylvania, 15705, USA

20 ¹⁰Department of Earth Sciences - Geochemistry, Faculty of Geosciences, Utrecht University. PO Box 80021, 3508 TA Utrecht, Netherlands

¹¹Department of Earth and Environmental Sciences, University of Michigan, 48109, USA

¹²Geological Survey of Denmark and Greenland, 1350 Copenhagen, Denmark

25 ¹³School of Natural Sciences, Technology and Environmental Studies, Södertörn University, SE-14189 Huddinge, Sweden

¹⁴Polish Geological Institute-National Research Institute Krakow, 31-560 Krakow, Poland

¹⁵Christian-Albrechts-University, Institute of Geosciences, Department of Organic Geochemistry, 24118 Kiel, Germany

30 *Correspondence to:* Ulrich Kotthoff (ulrich.kotthoff@uni-hamburg.de)



Abstract

Sediment records recovered from the Baltic Sea during Integrated Ocean Drilling Program Expedition 347 provide a unique opportunity to study paleoenvironmental and -climate change in central/northern Europe. Such studies contribute to a better understanding of how environmental parameters change in continental shelf seas and enclosed basins. We present a multi-proxy-based reconstruction of paleotemperature (both marine and terrestrial), -salinity, and -ecosystem changes from the Little Belt (Site M0059) over the past ~8,000 years, and evaluate the applicability of inorganic and organic proxies in this particular setting.

Salinity proxies (diatoms, aquatic palynomorphs, ostracods, long chain diol index – LDI) show that lacustrine conditions occurred in the Little Belt until ~7,400 cal. yr BP. A connection to the Kattegat at this time can be excluded, but a direct connection to the Baltic Proper may have existed. The transition to the brackish-marine conditions (more saline and warmer) of the Littorina Sea stage occurred within ~200 yr when the connection to the Kattegat became established (~7,400 cal. yr BP). The different salinity proxies used here show similar trends in relative changes in salinity, but do often not allow quantitative estimates of salinity. The reconstruction of water temperatures is associated with particular large uncertainties and variations in absolute values by up to 8 °C for bottom waters and even up to 16 °C for summer surface waters. Concerning the foraminiferal Mg/Ca reconstruction, contamination in the deeper intervals may have led to an over-estimation of temperatures. Differences in results based on the lipid proxies (LDI and TEX₈₆) can partly be explained by the application of modern-day proxy calibrations in areas which experienced significant changes in depositional settings, in case of our study e.g. change from freshwater to marine conditions. Our study shows that particular caution has to be taken when applying and interpreting proxies in coastal environments, where water mass conditions can experience more rapid and larger changes than in open-ocean settings. Approaches using a multitude of independent proxies may thus allow a more robust paleoenvironmental assessment.

1 Introduction

Coastal marine environments are particularly susceptible to global climate change (IPCC, 2014). With ongoing climate change, sea water is warming, and together with circulation changes and human-induced eutrophication this results in decreasing dissolved oxygen concentrations in many areas worldwide (Keeling and Garcia, 2002; Meier et al., 2012). This is particularly the case in semi-enclosed basins such as the Gulf of Mexico (Osterman et al., 2005; Platon et al., 2005), (Scandinavian) fjords (Gustafsson and Nordberg, 2000; Filipsson and Nordberg, 2004), and the Baltic Sea (Diaz and Rosenberg, 2008; Conley et al., 2011; Gustafsson et al., 2012). Climate change in recent decades is also showing a persistent trend to a more positive state of the North Atlantic Oscillation resulting in wetter conditions especially over northern Europe (Hurrell, 1995; Visbeck et al., 2001). Increased westerly winds together with a changed barotropic pressure gradient would lead to increased inflows of



saline water into the Baltic Sea. Furthermore, the increase in continental runoff due to increased precipitation may result in a freshening of the Baltic Sea (Matthäus and Schinke, 1999; Gustafsson and Westman, 2002).

Both temperature and salinity changes will have important consequences for the Baltic Sea environment (e.g. Meier et al., 2012). To improve our understanding of the impact and magnitude of future environmental change in the Baltic Sea region, it is advantageous to generate high-resolution paleo-reconstructions to investigate how salinity and temperature varied in the past (e.g. Zillén et al., 2008; Andrén et al., 2015a). A multi-proxy approach, comprising proxies representative for bottom water, surface water and air (terrestrial) conditions, allows us to reconstruct a wide array of environmental change (especially temperature and salinity) from the same samples, and thus, how conditions simultaneously changed with the same age constraints.

The occurrence of specific species of ostracods and foraminifera are important indicators of bottom water parameters, in case of the Baltic Sea primarily salinity (Lutze, 1965; 1974; Murray, 2006; Frenzel et al., 2005; 2010; Viehberg et al., 2008). Additionally, stable oxygen and possibly carbon isotopes in foraminifera are commonly related to changes in salinity, though stable oxygen isotopes are also influenced by temperature and global ice volume, while productivity is another control factor for carbon isotopes (Kristensen and Knudsen, 2006, Filipsson et al., in press). Bottom water temperatures (BWT) can be reconstructed using Mg/Ca in benthic foraminifera (Raitzsch et al., 2008), but the specific conditions in the Baltic Sea may significantly influence the application of Mg/Ca (Groeneveld and Filipsson, 2013).

A proxy which appears to be only dependent on temperature and may therefore be ideal for the Baltic Sea are clumped isotopes on molluscs. This proxy has not yet been applied to samples from the Baltic Sea. 'Clumped isotopes', or, more correctly, 'clumped isotopologues', are isotopic molecules that contain more than one rare isotope (for example, the carbonate isotopologue $\text{Ca}^{13}\text{C}^{18}\text{O}^{16}\text{O}_2$). The abundance of these molecules in carbonate is determined by the formation temperature of the mineral.

Due to the low salinity and overall shallowness of the Baltic Sea, planktonic foraminifera are absent from the Baltic Sea (Andrén et al. 2015a). Diatoms and marine palynomorphs like dinoflagellates, however, are common and often very good indicators of changes in salinity (Andrén et al., 2000; Snoeijs and Weckström, 2010; Ning et al., 2015).

The lipid paleothermometer TEX_{86} (TetraEther index of tetraethers consisting of 86 carbon atoms) and its derivatives (Schouten et al., 2002; Kim et al., 2010) is frequently used to reconstruct SSTs. In the Baltic Sea, the TEX_{86}^L has been shown to correlate well with summer SSTs and it has been used to investigate climate driven changes in SST over the past ~1,000 yr (Kabel et al., 2012). A more recently introduced proxy that shows promise in paleoenvironmental studies is the LDI (Rampen et al., 2012). This proxy makes use of the sedimentary distribution of long chain diols (LCDs) synthesized by eustigmatophytes and in different marine settings has been suggested to either reflect an annual (Rampen et al., 2012; de Bar et al., 2016) or a summer SST signal (Lopes dos Santos et al., 2013). In addition to SST, however, salinity has been observed to also affect the distribution of LCDs in aquatic environments (Versteegh et al., 1997). Terrestrial palynomorphs such as pollen grains are ideal biotic proxies for the reconstruction of continental environmental and climate dynamics. Techniques such as the modern



95 analogues technique (MAT) furthermore allow calculating quantitative climate data (e.g. temperature, precipitation, seasonality) from pollen assemblages (e.g. Guiot, 1990; Kotthoff et al., 2008, 2011).

Despite a large amount of proxy-based research performed in the Baltic Proper (e.g. Zillén et al., 2008, Kotilainen et al. 2014), there are no continuous high-resolution records from the Baltic Sea and its connections to the Kattegat (Little Belt, Great Belt, and Öresund) surpassing ~20 m sediment length (Andrén et al., 2009; Bennike and Jensen, 2011). Such records would enable
100 multi-proxy studies in high temporal resolution for the entire Holocene and possibly further back in time. Continuous high-resolution records would not only allow correlation between the different basins in the Baltic Sea region but also provide a connection to terrestrial archives and moreover to Greenland ice core records and marine records from the North Atlantic.

International Ocean Drilling Program (IODP) Expedition (Exp.) 347 drilled a series of long, continuous sediment records in the Baltic Sea region (Andrén et al., 2015a, b). Here we present a centennial-resolution multi-proxy study of IODP Exp. 347

105 Site M0059 from the Little Belt, one of the connections between the Baltic Sea and the North Sea using a variety of different proxies which are commonly used in paleoceanography to reconstruct past sea water temperature and salinity. We investigate how these proxies perform in a proximal setting like the Little Belt and how they link to seasonality. We selected the last ~8,000 yr of Site M0059 (top ~53 m of sediment) to include the transition from freshwater to brackish/marine conditions creating the connection between the Baltic Proper and the Kattegat. We show that a multi-proxy approach allows to unravel
110 the different factors which have influenced past conditions in the Little Belt, suggesting that its history may have been partly different from that of the Baltic Proper.

2 Regional settings and methods

2.1 Regional setting

The Baltic Sea, including the Gulfs of Bothnia, Riga and Finland, covers an area of 33,793 km² and spans a distance from the
115 53° to 66°N latitude (Leppäranta and Myrberg, 2009; Fig. 1). The Belt Sea, including the Öresund, the Great Belt, and the Little Belt, connects the Baltic Sea to the North Sea, through the Kattegat and Skagerrak. The Baltic Sea is one of the world's largest brackish water bodies, with a surface water salinity ranging from close to zero in the innermost parts of the Gulf of Finland, seven in the Baltic Proper and between 8 and 24 in the Belt Sea. A halocline, varying between 20 and 80 m water depth in the different subbasins, separates the upper water mass from more saline bottom water. The mean water depth is 54
120 m, varying between 25 and 200 m with the deepest basin, the Landsort Deep (central Baltic Sea) reaching a depth of 459 m (e.g. Leppäranta and Myrberg, 2009). The Baltic Sea basin is surrounded by two biomes, from temperate forest with mixed coniferous and broad-leaved trees in the south to boreal forest with taiga-like conditions in the north.

As one of the three straits connecting the Baltic Proper to the Kattegat, currents in the Little Belt consist of either relatively low salinity (14-17) water flowing out of the Baltic Sea into the Kattegat or higher salinity (>24) currents flowing into the
125 Baltic Sea. Because the Baltic Sea has a surplus of freshwater input, i.e. the input of water by precipitation and rivers exceeds



evaporation, a positive barotropic pressure gradient exists between the Baltic Proper and the Kattegat, so that under normal conditions surface waters flow from the Baltic Proper into the Kattegat (HELCOM, 1986; Jakobsen and Ottavi, 1997). The contribution of transport through the Little Belt is minor (<10%) in comparison with the Great Belt and the Öresund (Jacobsen, 1980). Occasionally the surface flow reverses and more saline water enters over the sills into the straits (Matthäus and Schinke, 1999; Mohrholz et al., 2015). The higher salinity causes the inflowing water to sink and continue as subsurface water into the Baltic Proper. This contrast in salinity results in a strongly stratified water column. However, because the Little Belt is very narrow, with high current velocity and turbulence, a major marine inflow from the Kattegat can lead to mixing of the water column (Jakobsen and Ottavi, 1997).

Mean surface water salinity in the Little Belt was 15.9 ± 0.4 for a 10-yr period (2004-2014), varying between 14.2 ± 0.9 in spring and 17.6 ± 1.5 in autumn, while mean bottom water salinity was 23.6 ± 1.0 varying between 21.5 ± 0.9 in winter and 25.2 ± 1.1 in summer (ICES, 2017). In the Little Belt region, the mean annual SST - averaged over a time interval from 2004-2014 - is 10.6 ± 0.6 °C (ICES, 2017). The mean winter SST is 2.5 ± 1.5 °C, while the mean summer SST is 17.6 ± 0.7 °C with maximum water temperatures of 21-22 °C observed from late July to mid-August (ICES, 2017). Bottom water temperatures average 7.6 ± 0.6 °C and vary between 4.3 ± 0.7 °C in winter and 9.3 ± 1.3 °C in summer (ICES, 2017).

The Baltic Sea region has experienced several climate-driven hydrological changes during the Holocene. Its history is highly dynamic and governed by the regional isostatic rebound and global sea level changes resulting in alternating freshwater and brackish phases and complex shoreline development (e.g. Björck, 1995, 2008; Knudsen et al., 2011; Andrén et al., 2011). The time interval investigated in this study comprises the transition from freshwater conditions to the brackish-marine conditions of the Littorina Sea stage. In the Baltic Proper, the Baltic Ice Lake (~16,000 to ~11,700 cal. yr BP) was followed by the brackish Yoldia Sea stage (~11,700 to ~10,700 cal. yr BP), the lacustrine Ancylus Lake stage (~10,700 to 10,200 cal. yr BP), a transitional low salinity phase and finally by the Littorina stage (e.g. Andrén et al. 2000; Sohlenius et al., 1996; Björck, 2008; Andrén et al., 2011).

2.2 Material and methods

During IODP Exp. 347, cores were recovered from five holes (A to E) at Site M0059 (Little Belt; Fig. 1), at ~37 m water depth ($55^{\circ}0.29'N$, $10^{\circ}6.49'E$). The results of our multi-proxy analyses are based on sediments from Holes A, C, D, and E.

2.2.1 Sedimentology and age model

The sedimentology of Holes M0059A, D, and E was assessed in the framework of the IODP Exp. 347 onshore science party (Andrén et al., 2015a, b). The sedimentary sequence of Site M0059 has been divided into seven lithostratigraphic units based on visual core descriptions and smear slide analyses (Andrén et al., 2015a). Only subunits Ia and Ib have been investigated in the present study. Subunit Ia (0-49.37 meters composite depth – mcd) is composed of mostly homogeneous black to greenish



black clay, with some millimetre-scale laminations. It was deposited under brackish-marine conditions, as indicated by diatom assemblages (Andrén et al., 2015a; Fig. 2). Subunit Ib (49.37–53.57 mcd) is a downhole continuation of Subunit Ia. Its base consists of 10–15 cm of black laminated clays. The remainder of Unit Ib comprises greenish to gray, silty clay, intercalated by centimetre-scale pale green laminae. Silt and the presence of freshwater diatoms indicate lacustrine conditions (Andrén et al., 2015a, Fig. 2). Magnetic susceptibility data (supported by natural gamma ray and gamma ray attenuation density data) collected from Holes M0059A–M0059E were used to correlate between each hole and to construct a composite section for Site M0059 including a meters composite depth (mcd) scale (Andrén et al., 2015a). This scale is used in this study. The age model for Site M0059 is based on 16 radiocarbon dates taken from bivalve fragments and intact bivalve specimens (*Abra alba*, *Macoma balthica*). Age-depth modelling was performed with CLAM (version 2.2; Blaauw, 2010) with 2000 iterations using the Marine13 calibration dataset (Reimer et al., 2013) and with a deviation (ΔR) of -90 ± 53 from the Marine13 reservoir age. A detailed description is given by Van Helmond et al. (accepted). Below 48.64 mcd, the ages have been extrapolated. In order to confirm the precision of the ^{14}C -based age model, we have biostratigraphically compared the marine pollen record from Site M0059 (Fig. 2; see below) with a pollen record from varved sediments in Lake Belau in northern Germany (Dörfler et al., 2012).

2.2.2 Geochemistry

In order to measure the total organic carbon (TOC) content, sediment samples from Holes C and E were freeze-dried, powdered and homogenized using an agate mortar and pestle. About 0.3 g of powdered sediment per sample was decalcified using 1M HCl. Subsequently the samples were washed repeatedly with milliQ water after which they were dried for 72 h at 60 °C. Finally the samples were powdered and homogenized again, after which they were measured using a Fisons Instruments NA 1500 NCS analyser at Utrecht University, the Netherlands. Results were normalized to international standards and TOC was calculated upon correction for weight loss by decalcification. The average analytical uncertainty of 0.07 wt.% was calculated based on duplicate analysis of sediment samples.

2.2.3 Palynology and pollen-based quantitative climate reconstructions

For the analysis of terrestrial and marine palynomorph assemblages, 36 samples were taken from 0 to ~53 mcd. Per sample, 1 to 6 g of sediment was processed using standard palynological techniques for marine sediments (e.g. Kotthoff et al., 2008). Whenever possible, >200 terrestrial palynomorphs (excluding spores and bisaccate pollen grains) were determined and counted per sample under 400 to 1000x magnification. In addition, organic-walled dinoflagellate cysts (dinocysts; as indicators for marine conditions; e.g. Zonneveld and Pospelova, 2015) and freshwater algae (as indicators for freshwater influence; e.g. Mudie et al., 2002) were determined and counted when occurring. We did not aim at counting a certain sum of dinocysts per



samples, since their absolute amount varied greatly over the analysed interval. On average, 50 dinocysts were identified per sample. This relatively low value is explained by the rarity of the counted types in some samples and relatively low dinocyst

190 diversity in the Baltic Sea (e.g. Ning et al., 2016).

Quantitative climate data were calculated from pollen data using the Modern Analogue Technique (MAT; e.g. Guiot, 1990). For this technique numerical methods are used to identify recent analogues for fossil pollen assemblages (e.g. Guiot, 1990; Kotthoff et al., 2008; 2011). Climate conditions for the best modern analogues are considered to be most similar to the conditions during which the fossil pollen assemblage was deposited. The MAT reconstructions are based on a database with
195 >3500 modern pollen spectra from Europe (Bordon et al., 2009) and the Mediterranean area (Dormoy et al., 2009). Here we used the ten modern assemblages with smallest chord distances for the reconstructions of the climate parameters. Bisaccate pollen was removed from the evaluated samples and the database due to its over-representation in marine pollen records (e.g. Kotthoff et al., 2008).

2.2.4 Diatoms

200 Sediment samples (36 in total) for the analysis of diatoms were freeze-dried. Subsequently, a known mass of sediment, between 0.03 and 0.07 g dry weight, was subsampled from selected depths and treated according to Warnock and Scherer (2015). Briefly, sediments were cleaned with dilute HCl to remove carbonates and 10 % H₂O₂ to remove organic carbon. The resultant sediment slurry was disbursed in a 2 L square cross-section beaker containing distilled water and a small glass table with known area including a coverslip, allowing for ultimate abundance determination. Coverslips were dried and permanently
205 mounted to glass slides with the mounting media Naphrax (refractive index = 1.65).

Each slide was counted to a minimum of 300 vegetative diatom valves. Absolute diatom abundance (ADA) can be calculated by counting the number of fields of view needed to reach 300 diatoms and scaling the number of diatoms counted in that known area relative to the total amount of surface area the sample settled onto and the original dry weight of the sediment sample (Warnock and Scherer, 2015). Diatoms were identified to the species level according to Snoeijs et al. (1993-1998),
210 Krammer and Lange-Bertalot (1986-1991), and Patrick and Reimer (1966). The salinity preferences and life forms (benthic or pelagic) of diatoms were classified according to Snoeijs et al. (1993-1998). All slides were analysed using differential interference contrast at 1000x magnification and oil immersion. *Chaetoceros* resting spores (CRS) were counted, but not identified to the species level and were not included in the absolute diatom abundance calculations for this study. Analysis of variance (ANOVA) was used to evaluate the differences between the means of these data, accompanied by a Tukey-Kramer
215 test to evaluate pair-wise relationships (for all statistical tests $\alpha = 0.05$). Because data derived from sediment cores is inherently chronological the results of pairwise tests are only reported for adjacent environment zones (EZs). All statistical relationships were evaluated using PAST v. 3.10 (Hammer et al., 2001).



2.2.5 Benthic Foraminifera

Thirty-six samples of 2-cm sediment thickness (20 ml sediment) were prepared for foraminiferal analyses and wet-sieved through sieves with 63, 100 and 1000 μm mesh. Each fraction was subsequently dried at 40 °C and weighed. The 100-1000 μm fraction was used for the foraminiferal assemblage analysis. In samples with a high concentration of mineral grains, the 100-1000 μm fraction of the samples was subjected to heavy liquid treatment using the heavy liquid tetrachlorethylene (C_2Cl_4) with a specific gravity of 1.6 g/cm^3 to separate foraminiferal tests from mineral grains prior to analysis. To ensure statistical validity of the assemblages, a minimum of 300 individual foraminifera were counted from each sample, when possible. Benthic foraminifera were counted and identified to species level to characterise the faunal assemblages. The benthic foraminiferal concentrations were calculated as number of specimens/ cm^3 sediment.

2.2.6 Ostracods

Since ostracod material was not abundant enough at Site M0059 to produce reliable percentage data, we used the total abundance of ostracods per 30- cm^3 sample. We divided the ostracods into predominant ecological groups and taxa and used their ecological data to reconstruct paleosalinity. A total of 75 30- cm^3 sediment samples were processed for ostracod analysis. Samples were freeze-dried and washed over a 63- μm sieve and subsequently oven dried in paper filters at 40–50 °C. Ostracods were picked from the entire sample residues and their valves identified and counted.

Two ecological classes of ostracods in relation to salinity were distinguished based on ecological data and distribution of modern taxa in the Baltic Sea and adjacent areas (Frenzel et al., 2010): freshwater and brackish-marine. Among brackish-marine ostracods very shallow and deeper water species were distinguished based on ecological data (Frenzel et al., 2010). Predominance of a very shallow water group implies salinity above 6-10, and an environment such as a lagoon, estuary or very shallow water open sea. The deeper-living ecological group includes species that can be found in the open sea environments at both very shallow and deeper locations with salinity > 7-14.

2.2.7 Stable isotopes in foraminifera

Stable oxygen and carbon isotope ($\delta^{18}\text{O}$, $\delta^{13}\text{C}$) measurements for 36 samples were performed on 10-20 specimens (100-1000 μm fraction) of *Elphidium selseyense* and *E. incertum*. The analyses were performed on a Finnigan MAT 251 gas isotope ratio mass spectrometer equipped with a Kiel I automated carbonate preparation device at the MARUM, University of Bremen, Germany. The stable isotopic data were calibrated relative to the Vienna Pee Dee belemnite (VPDB) using the NBS19 standard. The standard deviation of the house standard (Solnhofen limestone) over the measurement period was 0.03 ‰ for $\delta^{13}\text{C}$ and 0.06 ‰ for $\delta^{18}\text{O}$.



2.2.8 Trace metal/calcium in foraminifera

Up to 40 specimens (>150 µm) of *E. selseyense* and 25 specimens of *E. incertum* (>150 µm) were selected for trace metal/calcium analysis. If the number of specimens was not sufficient, both species were combined. Due to poor preservation, not enough specimens were present for the analysis of Mg/Ca ratios in depths <5 and >30 mcd. Trace metal/Ca in foraminifera from the Nordic/Baltic Seas has been shown to be affected by diagenetic coatings (Groeneveld and Filipsson, 2013; Ezat et al., 2016). Standard cleaning procedures for trace metal/Ca in foraminifera after clay removal either involve only an oxidation step to remove organic matter (Barker et al., 2003) or also include a reduction step before the oxidation (Martin and Lea, 2002) to remove (oxy)hydroxide coatings. Both methods, however, triggered a reaction on samples of Site M0059 which turned the foraminiferal fragments (dark) brownish. This suggests that an additional contaminating phase was present on the foraminiferal tests which was not removed by reduction but does respond to oxidation. A likely source for this are (Fe)-sulfides, which are easily formed in Baltic sediments including the Little Belt and adsorb cations (Raiswell and Canfield, 1998; Hardisty et al., 2016; Van Helmond et al., accepted). Oxidation would then turn the (Fe)-sulfide into an (Fe)-hydroxide, which has a brownish color. To remove this phase from the foraminiferal tests the standard combination of reduction and oxidation was reversed. First, oxidation was performed to form the hydroxide, followed by a reduction step to remove this again. As reducing agent 0.1 M hydroxylamine-hydrochloride buffered in a 1 M Na-acetate solution was used (Shen et al., 2001; Steinke et al., 2010). 250 µl reducing agent was added to the samples; the samples were heated for 30 min. at 70° C, and rinsed with Seralpur water three times. After cleaning, the samples were dissolved and centrifuged for 10 minutes (6000 rpm) to exclude any remaining insoluble particles from the analyses. The samples were diluted with Seralpur before analysis with Inductively Coupled Plasma-Optical Emission Spectrometry (ICP-OES; Agilent Technologies, 700 Series with autosampler ASX-520 Cetac and micro-nebulizer) at MARUM, University of Bremen, Germany. Instrumental precision was monitored after every five samples by analysis of an in-house standard solution with a Mg/Ca of 2.93 mmol/mol (standard deviation of 0.020 mmol/mol or 0.67 %). A limestone standard (ECRM752-1, reported Mg/Ca of 3.75 mmol/mol) was analysed to allow inter-laboratory comparison (Greaves et al., 2008; Groeneveld and Filipsson, 2013). The long-term average of the ECRM752-1 standard, which is routinely analysed twice after every 50 samples in every session, is 3.78 ± 0.073 mmol/mol. Analytical precision for *Elphidium* spp. was 0.08 % for Mg/Ca. Reproducibility using replicates of the same samples but cleaned separately was ± 0.17 mmol/mol (n = 18). Potential contamination was monitored using Al/Ca (clays), Mn/Ca, and Fe/Ca (both for diagenetic coatings) (see supplement for details).

2.2.9 Clumped isotopes in molluscs

The analyte for clumped isotope thermometry in the case of carbonate is CO₂ liberated by acid digestion, where Δ₄₇ is the measure of the amount of mass-47 isotopologues of CO₂ (primarily ¹³C¹⁸O¹⁶O) relative to that predicted by a random arrangement of atoms (Eiler, 2011a, b). A robust relationship between Δ₄₇ and the formation temperature of marine molluscs has been determined (Henkes et al., 2013). We measured the clumped isotope composition of mollusc material and report Δ₄₇



inferred temperatures for eleven samples. Mollusc material was separated from the sediment by wet sieving. A cold, ten-minute
soak of dilute H₂O₂ was used for samples where organic matter was particularly difficult to remove. All samples were triple-
rinsed in distilled water and hand cleansed with brushes under a microscope. After species identification, samples were ground
in a mortar and pestle and analysed at Johns Hopkins University (USA) on a Thermo Scientific MAT-253 isotope ratio mass
spectrometer coupled to an automated acid digestion and CO₂ purification system as described in Henkes et al. (2013). Samples
were analysed (3-7 replicates, as material permitted) alongside carbonate standards of varying composition and CO₂ gases
approaching equilibrium at 1000 °C and 30 °C, from January to March 2016 (see supplementary material). Measurements of
the temperature-equilibrated CO₂ gas samples were used to create an absolute reference frame for normalization of Δ₄₇ values
(Dennis et al., 2011), with the calculations performed using a MATLAB® script that accounts for temporal drift in analytical
conditions (Passey et al., 2010). Finally, we used the following empirically determined relationship between mollusc Δ₄₇ and
temperature (Henkes et al., 2013) to convert our measured Δ₄₇ to paleotemperatures: $\Delta_{47} = 0.0327 \times 10^6/T^2 + 0.3286$.

2.2.10 Biomarkers

A total of 40 sediments collected from Holes M0059A and M0059D was analysed for their lipid biomarker content. For this,
~1-5 gram of sediment was freeze-dried and extracted using a modified Bligh & Dyer technique (Rütters et al., 2002). An
aliquot of each Bligh and Dyer extract (~5 mg) was separated into an apolar and polar fraction using column chromatography
with activated Al₂O₃ as stationary phase and hexane:DCM (9:1, v/v) and DCM:MeOH (1:1) as respective eluents. The polar
fractions were subsequently dried under a gentle stream of N₂ and separated into two aliquots for analyses of glycerol dialkyl
glycerol tetraethers (GDGTs) and long chain diols (LCDs), respectively.
To analyse the GDGTs, aliquots of the polar fractions were dissolved in hexane:2-propanol (99:1; v/v) and passed through a
0.4 μm polytetrafluoroethylene (PTFE) filter. Analysis of GDGTs was performed using an Alliance 2695 (Waters, UK) high
performance liquid chromatograph (HPLC) coupled to a ZQ (Micromass, UK) single quadrupole mass spectrometer (MS) as
detailed in Zink et al. (2016) following the analytical protocols of Hopmans et al. (2000) and Liu et al. (2012). Isoprenoid and
branched GDGTs were detected using single ion recording of their protonated molecules [M+H]⁺ as outlined in Schouten et
al. (2013a). The TEX₈₆^L was calculated using the equation given by Kim et al. (2010):

$$\text{TEX}_{86}^{\text{L}} = [\text{GDGT-2}] / ([\text{GDGT-1}] + [\text{GDGT-2}] + [\text{GDGT-3}]) \quad [1]$$

TEX₈₆^L values were transferred to absolute temperatures using the Baltic Sea surface sediment calibration, which is best
correlated with summer SSTs (Kabel et al., 2012):

$$\text{SST} = 34.03 * \text{TEX}_{86}^{\text{L}} + 36.73 \quad [2]$$



310 In order to assess whether the $\text{TEX}^{\text{L}}_{86}$ can reliably be applied in our setting, we also calculated the branched isoprenoid tetraether (BIT) index (Hopmans et al., 2004):

$$\text{BIT} = ([\text{GDGT-1}] + [\text{GDGT-2}] + [\text{GDGT-3}]) / ([\text{Crenarchaeol}] + [\text{GDGT-1}] + [\text{GDGT-2}] + [\text{GDGT-3}]) \quad [3]$$

315 For the analysis of LCDs, we dissolved an aliquot of each polar fraction in DCM at a concentration of 2 mg ml⁻¹ and silylated the mixture by the addition of *N,O*-bis(trimethylsilyl)trifluoroacetamide (BSTFA) and pyridine and heating at 80 °C for 2 hours. Gas chromatography coupled to mass spectrometry (GC/MS) of LCDs was performed using an Agilent 7890A GC coupled to an Agilent 5975B MS following the method described in Rampen et al. (2012). LCDs were quantified using selected ion monitoring (SIM) of the masses *m/z* 313 (C₂₈ 1,13- and C₃₀ 1,15-diols) and *m/z* 341 (C₃₀ 1,13- and C₃₂ 1,15-diols). The
320 long chain diol index (LDI) was calculated and converted to SSTs using the equations provided by Rampen et al. (2012):

$$\text{LDI} = [\text{C}_{30} \text{ 1,15-diol}] / ([\text{C}_{28} \text{ 1,13-diol}] + [\text{C}_{30} \text{ 1,13-diol}] + [\text{C}_{30} \text{ 1,15-diol}]) \quad [4]$$

$$\text{LDI} = 0.033 \times \text{SST} + 0.095 \quad [5]$$

325 The Diol Index (DI) was calculated according to Versteegh et al. (1997):

$$\text{DI} = 100 * [\text{C}_{30} \text{ 1,15-diol}] / ([\text{C}_{30} \text{ 1,15-diol}] + [\text{C}_{32} \text{ 1,15-diol}]) \quad [6]$$

3 Results

3.1 Comparison of ¹⁴C age model with palynology-based chronology

330 The ¹⁴C-based age model for Site M0059 is discussed in detail by Van Helmond et al. (accepted). The mean sedimentation rate was ~6.5 mm/yr and there are no obvious signs of hiatuses in Unit I. A comparison with the varved high-resolution pollen record from Lake Belau in northern Germany (Dörfler et al., 2012; Figs. 1, 2), situated ~100 km south of Site M0059, reveals a close congruency between the pollen signals in the lacustrine and marine records. Particularly clear signals occurring in both Lake Belau and M0059 pollen records are the arrival of *Fagus* (beech) in the catchment area ~6,000 cal. yr BP, a characteristic
335 decline in *Ulmus* (elm) around ~5,600 cal. yr BP after preceding values between ~5 and ~10 %, maximum percentages of *Alnus* (alder) at ~5,200 cal. yr BP, and maximum percentages of *Fagus* at ~1,500 and ~600 cal. yr BP (Fig. 2 and Dörfler et al., 2012). Grains of cultivated Poacea taxa, i.e. cereals (Fig. 2), particularly *Triticum* (wheat) and *Secale* (rye), are consistently present after ~1,100 cal. yr BP and increase significantly after ~800 cal. yr BP. This signal is also congruent with the Lake Belau record, but the cereal pollen signal at Belau is stronger (Dörfler et al., 2012), probably due to higher agricultural activity
340 close to the lake. The general palynomorph preservation is excellent over the analysed interval, and pollen concentration varies



around 500 000 grains per gram sediment for most of the analysed samples. This is in accordance with the high TOC values (>2 wt%) encountered for most samples and between Holes (Fig. 2). Only in the uppermost part, pollen concentration decreases to values around 200 000 grains per gram.

3.2 Pollen-based climate reconstruction

345 The pollen-based climate reconstructions reveal a general increasing trend from ~8,000 to ~2,000 cal. yr BP in both annual precipitation and annual temperature (TANN Fig. 3, 4). The increase in the latter from ~5 to almost 9 °C is tied to an increase in coldest month temperatures (MTCO; ~-8 to almost 0 °C), while warmest month temperatures (MTWA) show a decreasing trend starting at ~7,000 cal. yr BP (~19 °C), which ends at ca. 2,000 cal. yr BP (~17 °C). Between ~2,000 and ~1,000 cal. yr BP, MTWA increase to >19 °C, and subsequently decrease again to <17 °C. The MTWA maximum around ~1,000 cal. yr BP
 350 is coeval with relatively low annual precipitation values (>640 mm compared to >800 mm earlier and subsequently).

3.3 Marine ecosystem changes

The Holocene record of Site M0059 was divided into four overall environmental zones (EZs; Table 1) based on statistically assessed changes in diatom assemblages (section 3.3.1) and coeval congruent signals of other marine proxies (benthic foraminifera – section 3.3.2, ostracods – section 3.3.4, and aquatic palynomorphs – section 3.3.5). While EZ1 is characterized
 355 by freshwater conditions, EZs 2-4 indicate brackish-marine depositional environments that persisted in the Baltic Sea during the Littorina Sea stage. EZ1 corresponds with lithological subunit Ib (49.37-53.57 mcd), while EZs 2-4 correspond with subunit Ia.

Table 1: Environmental zones of the Holocene records of Site M0059.

Zone	Depth (mcd)	Age (cal. yr BP)	Characteristics
EZ1	~53 to ~49	~7,800 to ~7,400	high absolute/relative values of freshwater proxies
EZ2	~49 to ~22	~7,400 to ~4,100	increased abundance of indicators of marine influence
EZ3	~22 to ~6	~4,100 to ~1,000	increase in diatom and <i>Chaetoceros</i> spore abundance, decreased indicators of marine influence
EZ4	~6 to top	~1,000 to present	increase in brackish diatoms, <i>Gymnodinium</i> cysts, decrease in diatom abundance

360

3.3.1 Diatoms

Relative abundances of salinity-based diatom assemblages, as well as absolute diatom abundance (ADA) plotted as the number of valves per gram dry weight of sediment (v/dgw), absolute abundance of *Chaetoceros* resting spores (CRS; v/dgw), and the



ratio of benthic to planktonic diatoms are presented on Figure 3. The division into four environmental zones (EZ) as described above was based on salinity preference, ADA, CRS abundance, and the ratio of benthic to planktonic diatoms (B:P). These are in general agreement with signals reflected by other proxies (see below).

EZ1 (~7,800 to ~7,400 cal. yr BP) is based on three diatom samples characterized by dominance of freshwater taxa, rare CRS abundance, (average 3.2×10^5), low ADA (average 2.5×10^7), and low B:P (0.48). EZ2 (~7,400 to ~4,100 cal. yr BP) is defined by a distinct increase in brackish and marine species at the expense of freshwater diatoms. In addition, there is a clear increase in the B:P ratio (average 4.17), ADA (average 4.65×10^7) and CRS absolute abundance (average 1.0×10^7). EZ2 contains both the highest B:P and the greatest range in values of B:P. EZ3 (~4,100 to ~1,000 cal. yr BP) shows an increase in marine, brackish-marine, and freshwater species at the expense of brackish species. The B:P ratio (average 2.65) declines some in EZ3, however ADA (average 5.1×10^7) and CRS absolute abundance (average 2.2×10^7) are highest in this interval compared to the rest of the core. Marine and brackish-marine species increase in abundance from the base of this zone to ~1,100 cal. yr BP concurrent with a decrease in brackish species. Both diatom and CRS absolute abundance increase from the base of this zone to ~1,200 cal. yr BP. B:P increases from the base of the zone to ~1,000 cal. yr BP.

EZ4 (~1,000 cal. yr BP to present) begins with an increase in brackish species. The relative abundance of marine and brackish-marine taxa, as well as B:P ratio (average 2.07) decline rather gradually throughout this interval, whereas ADA (average 2.0×10^7) and CRS abundance (average 5.3×10^6) decline rapidly at ~1,000 cal. yr BP and remain at low levels until the core-top. The significance of the differences between the four identified EZs were assessed in regards to the percent abundance of all five salinity affinities, as well as ADA, CRS abundance, and B:P. ANOVA reveals a significant difference between the means of all of these measures (Table S1 in Supplement). The Tukey-Kramer pairwise test was then used to evaluate the differences between individual EZs. Statistical differences between adjacent zones, representing change through time, are reported in Table S2 (Supplement). Pairwise statistical analysis reveals significant differences between EZ1 and EZ2 in terms of all ecological metrics with the exception of ADA. EZ2 and EZ3 can be distinguished statistically on the basis of the percent of diatoms with a brackish affinity, which decreases from EZ2 to EZ3, as well as CRS, which increases from EZ2 to EZ3. EZ3 can be significantly distinguished from EZ4 in terms of ADA and CRS abundance, both of which decrease. Finally, EZ3 does not have a significant change in salinity with respect to EZ4, however there is a shift in the species present between these zones.

3.3.2 Benthic foraminiferal assemblages

Benthic foraminifera are found in sediments covering the interval since ~7,400 cal. yr BP until today. The foraminiferal assemblages comprise very few species, with *Elphidium selseyense* (formerly named *E. excavatum* forma *selseyensis*; see Darling et al., 2016) being dominant. *Elphidium incertum* is also found throughout the entire core, while all other species occur only in specific intervals. In the lower part of EZ2, from ~7,400 to ~6,600 cal. yr BP, the foraminiferal assemblages are



characterised by very high frequencies of *E. incertum* and, around ~6,900 cal. yr BP, relatively high abundance of *Ammonia beccarii*. After ~6,600 cal. yr BP the relative abundance of *A. beccarii* is strongly reduced, while *E. incertum* continues to dominate and increases in abundance until ~5,700 cal. yr BP. During most of the interval since ~5,700 cal. yr BP (top zone EZ3 to zone EZ1), only *E. selseyense* and *E. incertum* are found consistently, with only minor, short-term occurrences of

400 *Elphidium albiumbilicatum* and *Elphidium magellanicum* at ~5,900 cal. yr BP and ~4,850 cal. yr. BP, as well as a short-term occurrence of *A. beccarii* at ~3,800 cal. yr BP. The samples representing the past ~460 cal. yr BP contain no or only very few foraminifera (*E. selseyense* and a few specimens of *E. incertum* and *E. albiumbilicatum*).

3.3.3 Benthic foraminifer isotopes and trace metal/calcium

405 Mg/Ca values reach numbers which are comparable to modern core top analyses of the same species (Groeneveld and Filipsson, unpublished data). Mg/Ca values before 4,000 cal. yr BP, however, are still relatively high, suggesting that the cleaning did not fully remove the contamination. Although FeS and FeS₂ are present in the studied sediments of Site M0059 (Van Helmond et al., accepted), it remains unclear what specific kind of sulfide would have been present on the foraminiferal fragments as Fe/Ca did not vary between the different methods (Fig. S1 in Supplement). Mean Mn/Ca was much lower for the

410 samples in the oxidation-reduction series (10.09 vs 14.81 mmol/mol; Table S3 in Supplement; Fig. S1 in Supplement), but these are still values which are much higher than commonly accepted for uncontaminated foraminiferal calcite (Barker et al., 2003). It is possible that the high Mn/Ca values are truly part of the primary foraminiferal calcite and relate as such to redox conditions in the sediment. Groeneveld and Filipsson (2013) showed Mn/Ca values as high as 10.58 mmol/mol in living specimens of *Globobulimina turgida* from the hypoxic zone in the Gullmar Fjord. For future work it may be required to

415 perform a second reduction step instead of just the one step performed here. The difference in average Mg/Ca between *E. selseyense* and *E. incertum* was not significant (1.52 vs 1.53 mmol/mol; Supplements), so for the remainder only results of *E. selseyense* are included, as they are of higher resolution. Mg/Ca values decrease from 2.96 mmol/mol at ~4,000 cal. yr BP to values between 0.62 and 1.10 mmol/mol between ~2,200–800 cal. yr BP (Fig. 4). As a species-specific calibration is absent for *Elphidium* spp., we employed the Mg/Ca-temperature calibration for *Melonis barleeanum*, which has been shown to give

420 reasonable temperatures for the Baltic Sea area (Kristjánsdóttir et al., 2007; Anjar et al., 2012). Calculated bottom water temperatures decrease from 10.9 °C at ~4,000 cal. yr BP to 0–4 °C between ~2,200 to ~800 cal. yr BP.

$\delta^{18}\text{O}$ values show an initial increase from -1.2 to 0.4 ‰ from ~7,400 to ~6,700 cal. yr BP. $\delta^{18}\text{O}$ average -0.2 ‰ for the interval ~7,400 to ~3,700 cal. yr BP and increase to an average of 0.4 ‰ afterwards, suggesting either a more gradual decrease in bottom water temperature, an increase in bottom water salinity, or both. $\delta^{13}\text{C}$ values increase from -3.2 ‰ at ~7,000 cal. yr BP

425 to -2 ‰ at ~5,000 to ~4,500 cal. yr BP. Afterwards values oscillate around an average of -1.3 ‰, suggesting improved ventilation of the water column (Supplements, Table S3).



3.3.4 Ostracods

Ostracod abundance was relatively low (~5 valves/30 cm³, 23 samples barren), but preservation was good in most samples.

- 430 EZ1 is entirely comprised of freshwater species. Abundant freshwater taxa *Candona* spp. and *Cytherissa lacustris* were identified in the interval between ~7,800 and ~7,500 cal. yr BP. The rest of the record contains marine and brackish-water ostracod taxa. The ostracod assemblages imply a subdivision of EZ2 (Fig. 3). EZ2a (~7,400 to ~6,800 cal. yr BP) is mainly represented with two shallow water taxa, *Palmoconcha* spp. and *Hirschmania viridis*. The abundance peak of shallow water taxa of 6 valves/30 cm³ is observed at ~7,000 cal. yr BP. EZ2b (~6,800 to ~3,600 cal. yr BP) contains both shallow water and
- 435 deeper-living taxa, with deeper-living taxa being slightly more abundant and showing two abundance peaks in this interval. In the lower part (~5,600 to ~6,800 cal. yr BP), a peak of 7 valves/30 cm³ is observed for deeper-living taxa at ~6,500 cal. yr BP. A short interval (~5,600 to ~5,300 cal. yr BP) is barren of ostracods. The upper part of the interval, ~3,600 to ~5,300 cal. yr BP, includes a deeper-living-taxa peak of 5 valves/30 cm³ at ~5,000 cal. yr BP. *Sarsicytheridea bradii*, *Cytheropteron latissimum* and *Elofsonella concinna*, *Robertsonites tuberculatus*, and *Paraciprideis* sp. are the dominant taxa in this interval.
- 440 These are typical representatives of Arctic/Boreal shallow water shelf faunas (Stepanova et al., 2007). Open sea environment and salinity of 14-16 and higher is expected for this group of species (Frenzel et al., 2010). Shallower water species like *Palmoconcha* spp. and *Leptocythere* spp. are the most abundant among shallow water taxa.
- EZ3 (~3,600 to ~1,000 cal. yr BP) is characterized by an overall increase in abundance and predominance of shallow water taxa (reaching a peak of 15 valves/30 cm³ at ~3,500 cal. yr BP). The most abundant taxa here are the shallow water genera
- 445 *Leptocythere* spp. and *Palmoconcha* spp. These taxa are present in the underlying EZ2, but become dominant here. These genera inhabit lagoons and open sea environments with salinity above 7-12. A short interval between ~2,600 and ~2,200 cal. yr BP is barren of ostracods.
- Uppermost EZ1 (covering the past ~1,000 yr) is marked by a decrease in the taxonomic diversity; it is almost solely represented by *Sarsicytheridea bradii*. *S. bradii* can be found in open sea environments and at a salinity as low as 7 (Frenzel et al., 2010).

450 3.3.5 Aquatic palynomorphs

- Percentages of dinocysts and freshwater algae (Fig. 3) are based on the total pollen sum (thus representing a dinocyst/pollen or a freshwater algae/pollen ratio, respectively). The freshwater algae *Pediastrum* and *Botryococcus* are present in the entire record, but values >3 % are only found at >7,700 cal. yr BP (Fig. 3). We have combined the dinocysts of phototrophic taxa belonging to gonyaulacoids into one group ("G-cysts"; predominately comprising *Protoceratium/Operculodinium*,
- 455 *Spiniferites*, and *Lingulodinium*), and microreticulate, gymnodinioid cysts of *Gymnodinium* in another. While not all *Gymnodinium* cysts were identified to species level, most of the encountered *Gymnodinium* cysts probably belong to *C. nolleri*. Cysts of heterotrophic taxa were generally rare within the samples. The G-cysts percentages are >3 % between ~7,800 and ~7,400 cal. yr BP (EZ1), but increase to > 5 % around ~7,400 cal. yr BP. Thereafter, values of this proxy stay rather constant at ~10 % until ~4,000 cal. yr BP (EZ 2). For the latest ~4,000 cal. yr BP, G-cysts percentages vary around 5 %, with particularly



low values around 500 cal. yr BP (EZ 4). *Gymnodinium* cf. *nolleri* cysts are almost completely absent until ~7,000 cal. yr BP, increase rapidly at ~6,800 cal. yr BP, but in the following decline and are almost absent at ~4,000 cal. yr BP. A second interval of high *Gymnodinium* cf. *nolleri* abundances occurs between ~3,000 and ~300 cal. yr BP, with maximum values at ~1,000 and ~200 cal. yr BP.

3.3.6 Mollusc clumped isotopes

Eleven mollusc shell fragments from Holes M0059A and D were used to generate clumped-isotope bottom-water temperatures. The species analysed were identified as *Abra alba*, *Arctica islandica*, *Corbula gibba*, and *Macoma balthica* (see Table S4 in Supplement). The oldest analysed mollusc is from EZ2 (~6,800 cal. yr BP) and the youngest analysed shell fragment from EZ4 (~140 cal. yr BP). Clumped-isotope-inferred temperatures range from ~2 °C to ~12 °C. Average temperatures from ~7,000 to ~4,000 cal. yr BP are ~9 °C (with ~11.8 °C and ~5 °C respective maximum and minimum temperatures) while temperatures in the past ~4,000 yr increase from ~2.1 °C to ~7.7 °C (Fig. 4).

3.3.7 Biomarkers

The Diol Index (DI) shows consistently low values of 55.2 ± 2.7 in EZ1 but rapidly increases to values of 90.5 with the establishment of brackish-marine conditions at the start of the Littorina Sea stage (Fig. 3). Thereafter, DI values gradually decline and show a minimum of 54.3 around ~4,000 cal. yr BP, after which values gradually increase again until ~3,000 cal. yr BP, where they peak at 80.1. In the following, the DI stays rather constant averaging 77 ± 3.0 for the remainder of the record with an exception found around ~700 cal. yr BP, at which the DI decreases to values as low as 61.7.

High $\text{TEX}_{86}^{\text{L}}$ -based SSTs of about 20 °C persist in EZ1 but they rapidly decrease to 16 °C at the base of EZ2 and thereafter slowly decline to 14 °C until ~4,000 cal. yr BP (Fig. 4). In the following, $\text{TEX}_{86}^{\text{L}}$ -SSTs gradually increase and cumulate in a peak SST of 26 °C around ~1,000 cal. yr BP, after which SSTs decline again and are at a minimum of 14 °C around ~300 cal. yr BP. The uppermost part of the record (<300 cal. yr BP) is characterized by increasing SSTs that maximize at 21.1 °C in the core top sample.

At a value of 0.80, the BIT in the freshwater interval of EZ1 is high (Fig. 4). With the establishment of brackish-marine conditions (base of EZ2), the BIT rapidly declines, however, and shows only little variation (0.29 ± 0.04) in the organic-rich deposits of the Littorina Sea stage.

The LDI-inferred SSTs are with 15.3 ± 1.4 °C comparatively low in EZ1 but they rapidly increase and show a maximum of 24.3 °C at the base of EZ2 (Fig. 4). Subsequently, LDI-based SSTs gradually decline and show a minimum of 15.9 °C at ~1,000 cal. yr BP that is followed by a short-lived warming event with peak temperatures of 20.8 °C around ~900 cal. yr BP. A second minimum in LDI-based SSTs is observed between ~800 and ~400 cal. yr BP, after which temperatures increase again to a value of 18.3 °C close to the core top.



4 Discussion

According to our results EZ2 to EZ4 represent the Littorina Sea stage, while EZ1 reflects an interval of freshwater conditions. This setting allows us to apply and test a wide array of sea water salinity proxies under widely variable conditions. Of the various proxies used, diatoms, dinocysts of phototrophic taxa, and the Diol index (DI) mainly reflect surface water conditions, while foraminifera and ostracods indicate changes in the bottom water. The complex climatic development during the Holocene in the Baltic Sea region (Björck, 1995; Andrén et al., 2008; Zillén et al., 2008) enables us to compare and validate several temperature reconstruction methods, with pollen reflecting terrestrial conditions, LDI- and TEX^L₈₆ indicating changes in the surface water, and mollusc clumped isotopes and foraminiferal Mg/Ca and δ¹⁸O allowing the reconstruction of bottom water conditions.

4.1 Salinity and productivity changes

All biological proxies indicate a phase of low salinity before ~7,400 cal. yr BP during EZ1; diatom and ostracod data suggest freshwater conditions and low productivity in the lowermost part of EZ1 (Fig. 3). Among the aquatic palynomorphs, remains of the green algae *Pediastrum* sp. and *Botryococcus* sp., together with low occurrences of marine dinoflagellate cysts compared to pollen grains, indicate a significant freshwater influence. These factors indicate that EZ1 represents a low productivity freshwater environment. Low diatom abundance and a freshwater flora, taken together with sedimentological data including laminated silty clay (Andrén et al., 2015a), imply a lacustrine environment in the area around Site M0059 during this interval. Likewise, the DI shows lowest values in this interval that are of the same order of magnitude reported from other lacustrine environments (Versteegh et al., 1997). Comparison with the varved pollen record from Lake Belau (Fig. 2; Dörfler et al., 2012) indicates that EZ1 is probably not older than ~9,000 cal. yr BP, as e.g. indicated by the presence of *Alnus* and *Ulmus* in the lowermost samples with ~5 %. This is corroborated by the constant temperature values indicated by both pollen- and TEX^L₈₆-based SST encountered at the transition from EZ1 to EZ2. Our findings are in congruence with those of Bennike and Jensen (2011) and Van Helmond et al. (accepted) who stated that during the early Holocene, a large lake developed in the southern part of the Little Belt.

Fully marine conditions in the southern Kattegat were already established by ~9,300 cal. yr BP (Bendixen et al., 2016), but not before ~7,300 cal. yr BP in the central Baltic Proper (Björck, 2008). This implies that during EZ1 the Little Belt may have been connected to the Baltic Proper, but not to the Kattegat. Bennike and Jensen (2011) suggested that the transition to brackish conditions started at ~8,500 cal. yr BP in the Little Belt, however the oldest dated marine shell from the Little Belt is dated to ~7,700 cal. yr BP (Bennike and Jensen, 2011), which is consistent with our findings.

The change to the more marine conditions in EZ2 occurred quickly, as already implied by Andrén et al. (2015b), since several proxies show a rapid decrease or disappearance of freshwater indicators (diatoms, green algae, ostracods). At the same time, salinity proxies indicate increasing salinity, e.g. by growing CRS abundance, as *Chaetoceros* requires brackish to marine conditions (Snøeijs et al., 1993-1998). Maximum abundances of dinocysts of phototrophic taxa occurred in EZ2, which are



coeval with abundance maxima at the southern and southeastern coast of Sweden found by Ning et al. (2015) and Yu and Berglund (2007), and in the Gotland and the Fårö Basins (Brenner, 2005, Willumsen et al., 2013).

525 Maxima in *Gymnodinium* cf. *nolleri* cysts between ~6,800 and ~4,300 cal. yr BP (~42 to ~25 mcd) may also indicate more saline conditions, though they may also be related to a temperature increase (e.g. Thorsen et al., 1995, Thorsen and Dale, 1997; see below). The *Gymnodinium* peak at ~6,800 cal. yr BP is to our knowledge not yet described from the Baltic Sea and seems not to have occurred farther eastwards (Brenner, 2005; Yu and Berglund, 2007; Ning et al., 2015). Thorsen et al. (1995) and Harland and Nordberg (2011) describe later *Gymnodinium* mass occurrences from the Skagerrak and the Kattegat, but
530 sediments of the appropriate age to find the peak at ~6,800 cal. yr BP in our record were not reached in the framework of their studies.

Increasing content of foraminifera per gram sediment within a short interval also point to a salinity increase, as well as the near disappearance of the foraminifera *A. beccarii* at ~6,600 cal. yr BP and the relatively high frequencies of *E. incertum* until ~5,700 cal. yr BP. *Ammonia beccarii* is a euryhaline species (Murray, 2006), but it increases in frequency in lower-salinity
535 environments in the Kattegat-Baltic Sea region (e.g. Lutze, 1974; Seidenkrantz, 1993). *Elphidium incertum* is a shallow infaunal species that favours sandy substrate, in brackish, inner shelf areas (salinity >25), where it is particularly frequent just below the halocline in stratified waters (Lutze, 1974; Darling et al., 2016). Foraminiferal- $\delta^{18}\text{O}$ values also point to increasing salinity. The following drop in *E. incertum* and consequent increase in *E. selseyense* in the upper part of this zone (EZ2) may potentially be ascribed to somewhat reduced bottom-water salinities, as *E. selseyense* is an opportunistic species that is
540 widespread in tidal to shelf areas with relatively large variations in temperature and salinity (Murray, 2006; Darling et al., 2016). As stable $\delta^{18}\text{O}$ values do not suggest a strong change in salinity between ~6,600 and 3,700 cal. yr BP, the shift in benthic foraminiferal fauna may also be linked to a reduction in bottom-water oxygenation, as *E. incertum* is also reported to require relatively high oxygen concentrations (Lutze, 1974; Murray, 2006). However, the results of Van Helmond et al. (accepted) indicate a significant reduction in bottom-water oxygenation only at the onset of this interval. Bottom water salinity change
545 was not as abrupt but gradual, thus in terms of ostracod fauna, EZ2 can be subdivided into two sub-zones, with the lower interval ~7,400 to ~6,800 cal. yr BP representing a transitional early marine stage environment with salinity above 10-14 and the second interval ~6,800 to ~3,900 cal. yr BP with salinity above 14-16. There was only little change in diatom-based primary productivity compared to EZ1. There is likely a deepening of the photic zone or shallowing of the water column as indicated by the sharp increase in B:P. A decreasing Diol Index and possibly also decreasing *Gymnodinium* percentages during the
550 second half of EZ2 imply slightly decreasing salinity between ~5,500 and ~4,100 cal. yr BP. The interval represented by EZ2 (~7,400 to ~4,100 cal. yr BP) is thus characterized by brackish to marine conditions with higher salinity at the onset of the Littorina Sea stage and slowly decreasing salinity afterwards, particularly in the surface water. Gustafsson and Westman (2002) regard this as the most marine period in the Baltic Sea in general and suggest that low precipitation could be the main cause for the increased salinity, which is in accordance with generally low precipitation values reconstructed via the MAT (<600 mm/yr excluding one sample until 4,000 cal. yr BP, compared to values from the late 20th century which are generally >600 mm/yr and often reach ~800 mm/yr, e.g. Omstedt et al., 1997).



At the transition between EZ2 and EZ3, salinity was probably lower for a short interval, as indicated by the low values of the DI and a short increase of *A. beccarii*. In EZ3 (~4,100 to ~1,000 cal. yr BP), the DI, diatom and benthic foraminiferal assemblages, benthic $\delta^{18}\text{O}$, and to some degree, ostracod occurrences (with particularly high values at ~3,500 cal. yr BP) indicate another increase in salinity between ~4,100 and ~3,000 cal. yr BP (with ostracod-based results suggesting salinities around 14–16), and diatoms imply that EZ3 includes another particularly marine phase of the Little Belt region recorded at Site M0059. Peak marine conditions, as indicated by diatom species' salinity affinities, occur from ~1,200 to ~1,000 cal. yr BP, at the transition to EZ4. This can be seen in the statistically significant decrease in brackish diatom species, while the proportions of marine and brackish-marine diatom species both increase throughout this interval. The Diol Index also shows particularly high values at the transition between EZ3 and EZ4.

Environmental Zone 3 shows B:P ratios which are statistically similar to EZ2, implying a deep photic zone or shallow water column (supported by a peak in shallow water ostracod taxa in EZ3) and high productivity at the seafloor. The highest recorded primary productivity, as indicated by ADA, CRS, and probably benthic foraminifera and ostracod abundances occurs within EZ3 as well (~1,700 cal. yr BP), during an interval of particularly high precipitation (and thus presumably increased runoff; Fig. 3, pollen-based reconstructions), while the peak salinity conditions at the transition to EZ4 are coupled with a significant decrease in annual precipitation. While there is no significant difference in ADA between EZ2 and EZ3, there is a significant difference between EZ1 and EZ3, showing the longer term increase in diatom-based primary productivity.

Following the peak marine interval, EZ4 (past ~1,000 cal. yr BP) begins with increases in brackish diatom taxa and decreases in marine and brackish-marine diatom species to the core-top. These species shifts are not statistically significant, however, implying that changes between EZ3 and EZ4 are related to primary productivity and nutrient conditions more than salinity shifts. But the Diol Index and *Gymnodinium* percentages also decrease at the same time. In case of *Gymnodinium*, the decrease could be tied to temperature changes (according to Thorsen and Dale, 1997, see below). Productivity decline from EZ3 to EZ4 is demonstrated by statistically significant decreases in ADA and CRS abundance. The uppermost diatom sample in this interval has the lowest recorded ADA as well as the lowest B:P of any brackish water interval. This sample (of almost recent age) likely represents modern human influence to the Baltic Sea, i.e. eutrophication. Eutrophication would cause a decline in overall diatom abundance, as diatoms are often replaced by cyanobacteria (O'Neil et al., 2012; Michalak et al., 2013) and dinoflagellates (Wasmund and Uhlig, 2003) in cases of high levels of eutrophication. This would lead to a shallowing of the photic zone resulting from sunlight being rapidly absorbed by cyanobacteria and dinoflagellates in the upper water column, as seen in the low B:P ratio. The relative and absolute amount of dinocysts is decreasing though in the uppermost palynology sample, thus denser sampling will be needed to highlight the human influence to the Baltic Sea ecosystems in future studies. Human influence is, however, indicated by the significant increase of pollen of cultivated Poacea taxa (Fig. 2), starting at ~1,000 cal. yr BP, with consistent occurrences since ~700 cal. yr BP. The coeval decrease of pollen of tree taxa like *Alnus* and *Fagus* may be an anthropogenic deforestation signal due to increased agricultural activity (Fig. 2).

The *Gymnodinium* maxima encountered in EZ3 and EZ4 are probably temporally related to mass occurrences of *Gymnodinium* in the eastern Kattegat as described by Harland and Nordberg (2011) for ~300 and ~2,000 cal. yr BP. The occurrence of



Gymnodinium cysts in the sediments from the Skagerrak/Kattegat are tied to warm water conditions according to Thorsen and Dale (1997), and this would be congruent with our findings that the maximum at the transition from EZ3 to EZ4 is coeval with the Medieval Warm Period and high temperatures indicated by most proxies, but not by the LDI-based temperature. However, while Thorsen and Dale (1997) assign the cysts to *G. catenatum*, Harland and Nordberg (2011) claim that the *Gymnodinium* cysts found in Holocene sediments from the Skagerrak and Kattegat rather belong to *G. nolleri* (in accordance with our results) and that the known mass occurrences may not be tied to high temperatures. Considering our findings, *Gymnodinium* mass occurrences may as well be tied to particularly high salinity as implied by the good correlation with other salinity proxies, e.g. the Diol index (which varies around values of ~80, Fig. 3).

EZ4 is characterized by a taxonomic diversity decrease in ostracods; this assemblage is almost solely represented by one species *S. bradii*, together with a decrease in juvenile percentage, it may imply an unfavourable environment, salinity increase, low oxygen conditions and dissolution and/or not in situ burial.

Taken together, the different salinity proxies give a consistent picture of how salinity in the water column changed in the Little Belt during the last 8,000 cal. yr BP, with freshwater conditions preceding ~7,400 cal. yr BP, a rapid increase in salinity afterwards, a decrease until the transition to EZ3 (until ~4,000 yr), a subsequent increase until ~3,000 yr BP and a decrease in EZ4. Precipitation (reconstructed via pollen assemblages) may have been one of the factors influencing salinity, particularly between ~8,000 and ~4,000 cal. yr BP. Slight discrepancies between the salinity proxies can be explained by a) differences between surface and bottom waters and b) additional factors influencing microfossil assemblages such as productivity and temperature. While qualitative estimates are congruent for most proxies, quantitative salinity estimates could only rarely be made in the framework of our study.

4.2 Temperature reconstructions

Inorganic (e.g. Mg/Ca and $\delta^{18}\text{O}$ of benthic foraminifera, clumped isotopes) and organic temperature proxies (e.g. TEX₈₆, LDI) have become indispensable tools in paleoenvironmental research as they provide quantitative information of past climate variations. Yet, proxy-based temperature estimates may vary significantly and/or show different trends even within the same sample set. This apparent mismatch between proxies severely complicates their application in paleoenvironmental and – climate research. Ideally, multiple proxies should therefore be used simultaneously to provide independent paleotemperature records.

Pollen-based reconstruction of seasonal and mean air temperature as well as estimates on surface water temperature variations using the TEX₈₆ and LDI are feasible for the entire record of Site M0059 but clumped isotope and Mg/Ca data are missing in particular from the freshwater interval reflected in EZ1 and in the lowermost section of EZ2 due to the lack of sufficient carbonaceous micro- and macrofossils. Despite the low resolution of some proxies, there is a certain degree of similarity in temperature trends observed across the different proxies used in this study. The pollen-based temperatures reconstructed for the two uppermost samples (comprising the past ~100 years) show an average value of ~0.1 °C for MTCO and of ~16.4 °C



for MTWA, which fits well with mean temperatures observed in Denmark during January ($\sim 1.5^{\circ}\text{C}$) and August ($\sim 17.2^{\circ}\text{C}$; Danish Meteorological Institute, 2017). The most complete temperature record is provided by the LDI, which indicates a rather constant summer SST of $\sim 14.6^{\circ}\text{C}$ in the lowermost part of EZ1 that is followed by a rapid temperature increase to maximum values of 24°C at the transition from EZ1 to EZ2 at $\sim 7,400$ cal. yr BP (Fig. 4). An interval of generally higher mean annual air and water temperatures has previously been described from other records of the Baltic Sea region such as Lake Flarken, Sweden (Seppä et al., 2005) or the Skagerrak (Butruille et al., 2017) and is consistent with the Holocene Thermal Maximum (HTM), a time period of warm summers in higher latitudes. The pollen-based temperature reconstructions imply that in the terrestrial realm, high summer temperatures were already established before $\sim 7,400$ yr BP, but that temperatures were very low during winter. In EZ2, the LDI and MTWA indicate a gradual and slow cooling trend by ~ 1 to 4°C towards the top of EZ2. On the contrary, the $\text{TEX}^{L_{86}}$ indicate a rapid cooling and rather constant temperatures of $\sim 15^{\circ}\text{C}$ throughout EZ2 with a trend similar to the clumped isotope record. The general order of magnitude of the pollen-based temperatures for EZ2 (~ 8 to $\sim 1.5^{\circ}\text{C}$ MTCO and ~ 17.5 to $\sim 19^{\circ}\text{C}$ MTWA) is in accordance with pollen-based climate reconstructions from, e.g. central Germany (Kühl and Moschen, 2012), and the general trends in all temperature reconstructions are congruent with trends reported by Davis et al. (2003) and Mauri et al. (2015) for western central/northern Europe. However, findings of pollen of thermophilous species in Danish records from the Boreal and Atlantic periods imply that winters should have been mild enough for these taxa (e.g. Iversen, 1944).

In EZ3, the LDI-SST, MTWA and Mg/Ca ratios suggest a continuation of the cooling that agrees with trends observed in other records (Seppä et al., 2005), while MTCO, TANN and the $\text{TEX}^{L_{86}}$ indicate a gradual warming that cumulates in maximum air and SSTs at the transition to EZ4 at $\sim 1,000$ cal. yr BP and therewith time equivalent to the MWP. In EZ4, the LDI- and $\text{TEX}^{L_{86}}$ -based SSTs are characterized by a rapid cooling with minimum temperatures of 14°C ($\text{TEX}^{L_{86}}$) and 17°C (LDI) observed at ~ 400 cal. yr BP, corresponding to the Little Ice Age. Such a cooling trend is also evident in all pollen-based temperature reconstructions. In contrast to the pollen record, however, the LDI and $\text{TEX}^{L_{86}}$ show a warming trend in the topmost samples with SSTs increasing above 20°C , which is of the same order of magnitude as modern water temperatures observed during late July to mid-August in the Little Belt (ICES, 2017).

Reconstructed absolute temperatures vary significantly between the different inorganic and organic proxies (Fig. 4). This is - to some extent - explained by the different realms the proxies reflect but even between the LDI and $\text{TEX}^{L_{86}}$ lipid paleothermometers, which are both considered to reflect summer SSTs in the Baltic Sea, significant deviations are observed. Such discrepancies have been previously reported for both proxies from subpolar (Rodrigo-Gámiz et al., 2015) to tropical regions (Jonas et al., in review) and were explained by differences in either the habitat depth and/or seasonality of the biological sources of both proxies. Long chain diols used to calculate the LDI are synthesized by eustigmatophyte algae (Volkman et al., 1992) that are oxygenic photoautotrophs and therefore the LDI should record SST. Indeed, the LDI-based SST in the sample closest to the core top is 18.3°C and therewith closely matches the summer SST of $17.6 \pm 0.7^{\circ}\text{C}$ observed in the Little Belt region (ICES, 2017). This finding is in accordance with the observation that the LDI reflects SST during the late summer-autumn season based on a comparison of LCD distribution patterns in globally distributed marine surface sediments and



monthly satellite SST data (Rampen et al., 2012). In addition to the marine realm, LCDs have also been observed in freshwater environments (Rampen et al., 2014). These authors noted a moderate linear correlation between summer temperatures and the LDI in a set of globally distributed lake sediments. Yet, the slope of LDI regression lines found in lacustrine and marine settings differs significantly, suggesting that the reconstruction of LDI-based SST may be flawed in settings of high riverine input of organic matter. Indeed, substantial offsets between LDI-based SSTs and satellite derived SSTs have been observed in front of the Tagus and Sado river mouths (Iberian Atlantic margin) with the LDI yielding SST that are up to 8 °C lower than measured average or summer SSTs (de Bar et al., 2016). The comparatively low summer SST values of on average $14.6 \pm 0.4^\circ\text{C}$ that are observed in the freshwater interval of EZ1 and the subsequent rapid increase in SST towards the base of EZ2 may, therefore, be a result of the significant changes from a freshwater to brackish-marine environment of the Little Belt rather than a true climate signal. This is corroborated by high relative proportions of 1,15-C₃₂ diol that indicates substantial contributions of LCDs from freshwater eustigmatophytes (Volkman et al., 1999; Rampen et al., 2014) and the lack of major changes in absolute temperatures based on the TEX₈₆^L lipid paleothermometer and pollen patterns across the EZ1/EZ2 boundary (Fig. 4). TEX₈₆^L-based SSTs vary from 12 to 26 °C (average of $17.1 \pm 3.5^\circ\text{C}$) with three distinct maxima observed at the transition from EZ1 to EZ2 (~7,500 to ~7,300 cal. yr. BP; $19.6 \pm 0.1^\circ\text{C}$) as well as at the base (~900 cal. yr BP; 25.9°C) and the top of EZ4 (present-day; 21.1°C). This present-day TEX₈₆^L-based water temperature is with 21.1°C close to SSTs observed in the Little Belt region during late July to mid-August (ICES, 2017). This suggests that the TEX₈₆^L reflects summer surface water temperatures in the Baltic Sea as previously also argued by Kabel et al. (2012), who observed the best correlation for GDGT distribution patterns in surface sediments of the Baltic Sea with average water temperatures from July to October. In terms of absolute temperature and overall trends, the TEX₈₆^L record is to some degree similar to the clumped isotope record but differs significantly from the LDI as well as other temperature-based profiles (i.e. pollen and Mg/Ca ratios of benthic foraminifera). A factor potentially complicating the reconstruction of TEX₈₆^L-based SSTs is the input of large quantities of soil-derived GDGTs (Weijers et al., 2006; Schouten et al., 2013b). A quantitative mean to determine the input of terrestrial organic matter to aquatic environments is the BIT with low values of this proxy (<0.1) indicating open marine conditions and high values being representative for terrestrial settings (<0.9; Hopmans et al., 2004). Empirical studies suggest that the TEX₈₆ and its derivatives do not allow a reliable reconstruction of SSTs if BIT values exceed a threshold of ~0.3 (Weijers et al., 2006; Zhu et al., 2011). BIT values in the Little Belt have an average of 0.29 ± 0.04 in EZ2-4, close to but still below this threshold. The TEX₈₆^L does, therefore, not seem to be biased by an allochthonous contribution of GDGTs. This is also supported by an absence of correlation between BIT and TEX₈₆^L values ($r^2 = 0.04$; $p > 0.001$), which is only to be expected if the terrestrial influence on the TEX₈₆^L is negligible (Schouten et al., 2013a). In fact, a very similar TEX₈₆^L temperature record, covering the last 1,000 cal. yr BP with temperature maxima during the MWP and Modern Hypoxic Period (MHP), has been reported from the Gotland Basin in the central Baltic Proper (Kabel et al., 2012), suggesting that the TEX₈₆^L indeed traces climate-driven variations in SST in the brackish-marine Littorina Sea stage. However, in EZ1 high BIT values of 0.87 indicate a higher contribution of terrestrial-derived GDGTs that may potentially confound the application of the TEX₈₆^L in the freshwater interval of the Little



690 Belt. Yet, TEX_{86} -SSTs in EZ1 and the immediately overlying marine-brackish sediments of EZ2 are largely similar and are in agreement with the reported warming in the Baltic Sea region during the HTM (Seppä et al., 2005; Krossa et al., 2017). Temperatures inferred from carbonate-clumped isotopes and Mg/Ca ratios of benthic foraminifera are largely similar to those observed during late summer in the Little Belt. Indeed, in temperate climate settings molluscs and benthic foraminifera precipitate carbonate only if environmental conditions permit, so shell geochemical proxies (such as carbonate clumped isotopes and Mg/Ca) tend to be skewed towards the seasons when growth is favourable (Filipsson et al., 2004; Austin et al., 2006; Schöne, 2008; Skirbekk et al., 2016). Despite temperatures which are within range of present day variability, the cleaning experiments on the foraminiferal calcite show that the 8°C decrease in BWT may not be realistic after all. It cannot be excluded that the foraminiferal tests were still contaminated by the presence of authigenic carbonates like for example rhodochrosite, which can also contain Mg, and which cannot be removed by the current cleaning methodologies. The occurrence of such

700 authigenic carbonate deposits in the Baltic Sea is common (Huckriede and Meischner, 1996; Andrén et al., 2015b; Hardisty et al., 2016; Van Helmond et al., accepted) and likely also affects foraminiferal tests (Groeneveld and Filipsson, 2013). Remaining contamination is also suggested by the significant correlation coefficient between Mg/Ca and Mn/Ca ($r^2 = 0.72$) after the oxidation-reduction cleaning. This suggests that especially the older part of the Mg/Ca record is contaminated. The presence of benthic foraminifera in EZ2-4 and their absence in EZ1 is related to salinity, i.e. foraminifera do not occur in

705 the freshwater setting of EZ1. The absence of foraminifera in the upper meters of the record (<5 mcd), however, is more likely due to poor preservation of the foraminiferal calcite. Similarly, the foraminiferal abundance decreases in EZ2, such that enough specimens were still present to perform stable isotopes analyses, but there were too few to perform reliable Mg/Ca analyses. Poor preservation may have been caused by the degradation of organic matter in the sediment, which led to lower pH values of the pore water such that dissolution of the foraminiferal tests took place.

710 5 Conclusions

In this study, we have investigated and compared how inorganic and organic temperature as well as salinity proxies perform in the coastal setting of the Little Belt with highly variable environmental conditions. Sediments deposited since ~8,000 cal. yr BP at Site M0059 were analysed to capture the transition from freshwater to marine conditions and thus to study the effect of facies change on proxy applications.

715 Our study demonstrates that a multi-proxy approach allows deciphering the various factors which have influenced past oceanographic conditions in the Little Belt. Between ~7,800 and 7,400 cal. yr BP, a direct connection of the Little Belt to the Baltic Proper may have existed as salinity-specific proxies indicate lacustrine conditions, while a connection to the Kattegat can be excluded. Water temperatures and salinities increased within 200 yr after the onset of the Littorina Sea stage at ~7,400 cal. yr BP. An interval of particularly saline conditions and high summer water and air temperatures followed, although both

720 salinity and water temperatures declined with increasing precipitation until ~4,000 cal. yr BP. After ~4,000 cal. yr BP, the



Little Belt witnessed decreasing temperatures during the warm season both in the marine and terrestrial realm, while salinity increased.

In addition, our study highlights the importance and value of a multi-proxy approach to reconstruct past oceanographic conditions. The different salinity proxies used here show generally similar trends in relative changes in salinity, but do not allow quantitative estimates of salinity (except for marine ostracods). In contrast, the reconstruction of temperatures is associated with particular large uncertainties and variations in absolute values by up to 8 °C for bottom waters and even up to 16 °C for summer surface waters. For example, different cleaning techniques for Mg/Ca in the foraminifera show different results which partly correlate with indicators for contamination especially in the deeper intervals studied. This suggests that the Mg/Ca of those samples is likely over-estimated, so that the decreasing trend in Mg/Ca and thus calculated BWT may not be as large. The differences in results based on the lipid proxies (LDI and TEX₈₆^L) can partly be explained with the application of modern-day proxy calibrations in areas which experienced significant changes in depositional settings (e.g. change from freshwater to marine conditions). Our study shows that particular caution has to be taken when applying and interpreting proxies in coastal environments, where water mass conditions can experience more rapid and larger changes than in open-ocean settings. Approaches using a multitude of independent proxies may thus allow more robust paleoenvironmental assessment.

6 Data availability

Data not enclosed in the supplementary will be uploaded to the PANGAEA database (LINK). Already uploaded are ostracod data (<https://doi.pangaea.de/10.1594/PANGAEA.873270>).

Acknowledgements.

This investigation used samples from IODP Expedition 347. Stephen Obrochta, Sofia Ribeiro, Ingo Feeser, and Walter Doerfler are gratefully acknowledged for insightful discussions and comments on the age model, dinoflagellate cyst taxonomy and ecology, and the Lake Belau pollen record. We thank the crew and scientific party of IODP Expedition 347 as well as the technical staff at MARUM, Bremen for their support during the expedition's off- and onshore phase. We thank technical support from the respective laboratories. This study was supported by the German Research Foundation (grants KO3944/6-1 to UK, and BA3841/5-1 to TB), the Carlsberg Foundation and Geocenter Denmark (grants to MSS and ORC). TA, JG, NQK, and HLF thank the Swedish research councils VR and FORMAS, the LAM Foundation, the Crafoord Foundation as well as the Center for Environmental and Climate Research at Lund University for funding. TA also received funding from The Foundation for Baltic and East European Studies.

Edited by:



Reviewed by:

References

- 755 Andrén, E., Andrén, T., Kunzendorf, H.: Holocene history of the Baltic Sea as a background for assessing records of human impact in the sediments of the Gotland Basin. *The Holocene*. 10, 687-702, 2000.
Björck S., Andrén T., Jensen J.B.: An attempt to resolve the partly conflicting data and ideas on the Ancylus-Litorina transition. *Polish Geological Institute Special Papers* 23, 21-25, 2008.
Andrén, T., Bitinas, A., Björck, S., Emelyanov, E., Harff, J., Houmark-Nielsen, M., Jakobson, M., Jensen, J.B., Jørgensen, B.B., Kotilainen, A., Knudsen, K.L., Lambeck, K., Moros, M., Spiess, V., Uścińowicz, S., Veski, S., Zelchs, V.: IODP Prospectus 672, 2009.
- 760 Andrén, T., Björck, S., Andrén, E., Conley, D., Zillén, L., Anjar, J.: The development of the Baltic Sea basin during the last 130 ka. In Harff, J., Björck, S. Hoth, P. (eds.): *The Baltic Sea Basin*, 75–97. Springer, Berlin, 2011.
Andrén, T., Jørgensen, B.B., Cotterill, C., and the Expedition 347 Scientists: Baltic Sea Paleoenvironment. *Proceedings IODP*, 347. College Station, TX (Integrated Ocean Drilling Program), doi:10.2204/iodp.proc.347.101.2015, 2015a.
Andrén, T., Barker Jørgensen, B., Cotterill, C., Green, S., IODP expedition 347 scientific party: Baltic Sea basin paleoenvironment and biosphere. *Scientific Drilling* 20, 1-12, doi:10.5194/sd-20-1-2015, 2015b.
Anjar, J., Adrielsson, L., Bennike, O., Björck, S., Filipsson, H.L., Groeneveld, J., Knudsen, K.L., Larsen, N.K., Möller, P.: Palaeoenvironmental history of the Baltic Sea basin during Marine Isotope Stage 3. *Quat. Sci. Rev.* 34, 81-92 2012.
- 770 Antonsson, K., Brooks, S.J., Seppä, H., Telford, R.J., Birks, H.J.: Quantitative palaeotemperature records inferred from fossil pollen and chironomid assemblages from Lake Giltjärnen, northern central Sweden. *J. Quaternary Sci.* 21, 831-841, 2006.
Austin, W.E.N., Cage, A.G., Scourse, J.D.: Mid-latitude shelf seas: a NW European perspective on the seasonal dynamics of temperature, salinity, and oxygen isotopes. *The Holocene* 16, 937-947, 2006.
Barker, S., Greaves, M., Elderfield, H.: A study of cleaning procedures used for foraminiferal Mg/Ca paleothermometry. *Geochem., Geophys., Geosys.*, 4, doi:10.1029/2003GC000559, 2003.
- 775 Bennike, O. Jensen, J.B.: Postglacial, relative shore-level changes in Lillebælt, Denmark. *Geol. Surv. Den. Green. Bull.*, 23, 37–40, 2011.
Björck, S.: A review of the history of the Baltic Sea, 13.0-8.0 ka BP. *Quatern. Int.* 27, 19-40, doi:10.1016/1040-6182(94)00057-C, 1995.
- 780 Björck, S.: The late quaternary development of the Baltic Sea Basin. in: *The BACC Author Team (Ed.), Assessment of Climate Change for the Baltic Sea Basin*. Springer-Verlag, Berlin-Heidelberg, pp.398–407, 2008.
Bendixen, C., Jensen, J.B., Boldreel, L.O., Clausen, O.R., Bennike, O., Seidenkrantz, M.-S., Nyberg J., Hübscher, C.: The Holocene Great Belt connection to the southern Kattegat, Scandinavia: Ancylus Lake drainage and Early Littorina Sea transgression. *Boreas*, doi: 10.1111/bor.12154, 2016.



- 785 Blaauw, M.: Methods and code for ‘classical’ age-modelling of radiocarbon sequences. *Quat. Geochronol.* 5, 5512-5518, 2010.
Bordon, A., Peyron O., Lézine A.-M., Brewer S., Fouache E.: Pollen-inferred Late-Glacial and Holocene climate in southern Balkans (Lake Maliq). *Quatern. Int.* 200, 19-30, 2009.
Brenner, W.W.: Holocene environmental history of the Gotland Basin (Baltic Sea) – a micropalaeontological model. *Palaeogeogr. Palaeoclimatol.* 220, 227–241, 2005.
- 790 Butruille, C., Krossa, V.R., Schwab, C., Weinelt, M.: Reconstruction of mid- to late-Holocene winter temperatures in the Skagerrak region using benthic foraminiferal Mg/Ca and $\delta^{18}\text{O}$. *The Holocene* 1, 63-721-10, doi:10.1177/0959683616652701, 2017.
Conley, D.J., Carstensen, J., Aigars, J., Axe, P., Bonsdorff, E., Eremina, T., Haahti, B.-M., Humborg, C., Jonsson, P., Kotta, J., Lännegren, C., Larsson, U., Maximov, A., Medina, M.R., Lysiak-Pastuszek, E., Remeikaite-Nikiene, N., Walve, J.,
- 795 Wilhelms, S., Zillén, L.: Hypoxia is increasing in the coastal zone of the Baltic Sea. *Envir. Sci. Tech.* 45, 6777-6783, 2011.
Danish Meteorological Institute: <http://www.dmi.dk/vejir/arkiver/normaler-og-ekstremer/klimanormaler-dk/vejirnormal/> visited 24.02.2017.
Darling, K.D., Schweizer, M., Knudsen, K.L., Evans, K.M., Bird, C., Roberts, A., Filipsson, H.L., Kim, J.-H., Gudmundsson, G., Wade, C.M., Sayer, M.D.J., Austin, W.E.N.: The genetic diversity, phylogeography and morphology of Elphidiidae
- 800 (Foraminifera) in the Northeast Atlantic. *Mar. Micropalaeontol.*, doi: 10.1016/j.marmicro.2016.09.001, 2016.
Dennis, K. J., Affek, H. P., Passey, B. H., Schrag, D. P., Castañeda I.S., Schouten, S.: A review of molecular organic proxies for examining modern and ancient lacustrine environments. *Quaternary Sci. Rev.* 30, 2851-2891, 2011.
Davis, B.A.S., Brewer, S., Stevenson, A.C., Guiot, J., Data Contributors: The temperature of Europe during the Holocene reconstructed from pollen data. *Quaternary Sci. Rev.* 22, 1701-1716, doi:10.1016/S0277-3791(03)00173-2, 2003.
- 805 de Bar, M.W., Dorhout, D.J.C., Hopmans, E.C., Rampen, S.W., Sinninghe Damsté, J.S., Schouten S.: Constraints on the application of long chain diol proxies in the Iberian Atlantic margin. *Org. Geochem.* 101,184-195, 2016.
Diaz, R. J., Rosenberg, R.: Spreading dead zones and consequences for marine ecosystems. *Science* 321, doi:10.1126/science.1156401, 2008.
Dörfler, W., Feeser, I., van den Bogaard, C., Dreibrodt, S., Erlenkeuser, H., Kleinmann, A., Merkt, J., Wiethold, J.: A high-
- 810 quality annually laminated sequence from Lake Belau, Northern Germany: Revised chronology and its implication for palynological and tephrochronological studies. *The Holocene* 22(12), 1413–1426, doi: 10.1177/0959683612449756, 2012.
Dormoy, I., Peyron, O., Combourieu Nebout, N., Goring, S., Kotthoff, U., Magny, M., Pross, J.: Terrestrial climate variability and seasonality changes in the Mediterranean region between 15 000 and 4000 years BP deduced from marine pollen records. *Clim. Past* 5, 615-632, 2009.
- 815 Eiler, J.M.: Defining an absolute reference frame for ‘clumped’ isotope studies of CO_2 . *Geochim. Cosmochim. Acta* 75, 7117-7131, 2011.
Eiler, J.M.: Paleoclimate reconstruction using carbonate clumped isotope thermometry. *Quaternary Sci. Rev.* 30, 3575-3588, 2011.



- Ezat, M.M., Rasmussen, T.L., Groeneveld, J.: Reconstruction of hydrographic changes in the southern Norwegian Sea during the past 135 kyr and the impact of different foraminiferal Mg/Ca cleaning protocols. *Geochem., Geophys., Geosyst.* 17, doi: 10.1002/2016GC006325, 2016.
- Filipsson, H.L., Nordberg, K.: Climate Variations, an overlooked Factor influencing the Recent Marine Environment. An Example from Gullmar Fjord, Sweden, Illustrated by Benthic Foraminifera and Hydrographic Data. *Estuaries* 27, 867-881, 2004
- Filipsson, H.L., Nordberg, K., Gustafsson, M.: Seasonal study of $\delta^{18}\text{O}$ and $\delta^{13}\text{C}$ in living (stained) benthic foraminifera from two Swedish fjords. *Mar. Micropaleontol.* 53, 159-172, 2004.
- Filipsson, H.L., McCorkle, D.C., Mackensen, A., Bernhard, J.M., Andersson, L.S., Naustvoll, L.-J., Caballero-Alfonso, A.M., Nordberg, K., Danielssen, D.S.: Seasonal variability of stable carbon isotopes ($\delta^{13}\text{C}_{\text{DIC}}$) in the Skagerrak and the Baltic Sea: Distinguishing between mixing and biological productivity. *Palaeogeogr. Palaeoclimatol.* doi.org/10.1016/j.palaeo.2016.11.031, 2016.
- Frenzel, P., Boomer, I.: The use of ostracods from marginal marine, brackish waters as bioindicators of modern and Quaternary environmental change. *Palaeogeogr. Palaeoclimatol.* 225, 68-92, 2005
- Frenzel, P., Keyser, D., Viehberg, F.A.: An illustrated key and (palaeo)ecological primer for postglacial to Recent Ostracoda (Crustacea) of the Baltic Sea. *Boreas*, 39(3):567-575. doi:10.1111/j.1502-3885.2009.00135.x, 2010. Greaves, M., Caillon, N., Rebaubier, H., et al.: Interlaboratory comparison study of calibration standards for foraminiferal Mg/Ca thermometry. *Geochem., Geophys., Geosyst.* 9, Q08010, doi:10.1029/2008GC001974, 2008.
- Groeneveld, J., Filipsson, H.L.: Mg/Ca and Mn/Ca ratios in benthic foraminifera: the potential to reconstruct past variations in temperature and hypoxia in shelf regions. *Biogeosciences* 10, 5125-5138, 2013.
- Guiot, J.: Methodology of palaeoclimatic reconstruction from pollen in France: *Palaeogeogr. Palaeoclimatol.* 80, 49-69, 1990.
- Gustafsson, M., Nordberg, K.: Living (stained) benthic foraminifera and their response to the seasonal hydrographic cycle, periodic hypoxia and to primary production in the Havstens Fjord on the Swedish west coast. *Estuar. Coast Shelf S.* 51, 743-761, 2000.
- Gustafsson, B.G., Westman, P.: On the causes for salinity variations in the Baltic Sea during the last 8500 years. *Paleoceanography* 17, doi:10.1029/2000PA000572, 2002.
- Gustafsson, B.G., Schenk, F., Blenckner, T., Eilola, K., Meier, H.E.M., Müller-Karulis, B., Neumann, T., Ruoho-Airola, T., Savchuk, O.P., Zorita, E.: Reconstructing the development of Baltic Sea eutrophication 1850-2006. *Ambio* 41, 534-548. doi:10.1007/s13280-012-0318-x, 2012.
- Hammer, Ø., Harper, D.A.T., Ryan, P.D.: PAST: Paleontological statistics software package for education and data analysis. *Palaeontol. Electron.* 4, 2001.
- Hardisty, D.S., Riedinger, N., Planavsky, N.J., Asael, D., Andrén, T., Jørgensen, B.B., Lyons, T.W.: A Holocene history of dynamic water column redox conditions in the Landsort Deep, Baltic Sea. *Am. J. Sci.* 316, 713-745, doi:10.2475/08.2016.01, 2016.



- Harland, R., Nordberg, K.: The identification, occurrence and importance of microreticulate dinoflagellate cysts in the latest Holocene sediments of the Skagerrak and Kattegat, west coast of Sweden. *Rev. Palaeobot. Palyno.* 164, 84-92, 2011.
- 855 HELCOM.: Water balance of the Baltic Sea. In: *Baltic Sea Environment Proceedings Vol. 16. The Baltic Marine Environment Protection Commission*, Helsinki, Finland, 1986.
- Henkes, G.A., Passey, B.H., Hopmans, E.C., Schouten, S., Pancost, R.D., van der Meer, M.T., Wanamaker, A.D., Grossman, E.L., Ambrose, W.G., Carroll, M.L.: Carbonate clumped isotope compositions of modern marine mollusk and brachiopod shells. *Geochim. Cosmochim. Ac.* 106, 307-325, 2013.
- 860 Hopmans, E.C., Schouten, S., Pancost, R.D., van der Meer, M.T.J., Sinninghe Damsté, J.S.: Analysis of intact tetraether lipids in archaeal cell material and sediments by high performance liquid chromatography/atmospheric pressure chemical ionization mass spectrometry. *Rapid Commun. Mass Sp.* 14, 585-589, 2000.
- Hopmans, E.C., Weijers, J.W.H., Schefuß, E., Herfort, L., Sinninghe Damsté, J.S., Schouten, S.: A novel proxy for terrestrial organic matter in sediments based on branched and isoprenoid tetraether lipids. *Earth Planet. Sc. Lett.* 224, 107-116, 2004.
- 865 Huckriede, H., Meischner, D.: Origin and environment of manganese-rich sediments within black-shale basins. *Geochim. Cosmochim. Ac.* 60, 1399-1413, 1996.
- Hurrell, J.W.: Decadal trends in the North Atlantic Oscillation: Region Temperatures and Precipitation. *Science* 269, 676-679 doi:10.1126/science.2695224.676, 1995.
- ICES Hydrochemistry, CTD and Bottle data portal. ICES, Copenhagen, 2017.
- 870 Jakobsen, F., Ottavi, J.: Transport through the contraction area in the Little Belt. *Est., Coast., Shelf Sci.* 45, 759-767, 1997.
- IPCC, 2014: *Climate Change 2014: Synthesis Report. Contribution of Working Groups I, II and III to the Fifth Assessment Report of the Intergovernmental Panel on Climate Change* [Core Writing Team, R.K. Pachauri and L.A. Meyer (eds.)]. IPCC, Geneva, Switzerland, 151 pp.
- Iversen, J.: *Viscum, Hedera and Ilex as Climate Indicators*. *Geol. Foren. Stock. For.* 66, 463-483, 1944.
- 875 Jonas, A.S., Schwark, L., Bauersachs, T.: Late Quaternary sea surface temperature variation of the Northwest Pacific Ocean based on the lipid paleothermometers TEX^H₈₆, U^{K'}₃₇ and LDI. *Deep Sea Research II*, in review.
- Kabel, K., Moros, M., Porsche, C., Neumann, T., Adolphi, F., Andersen, T.J., Siegel, H., Gerth, M., Leipe, T., Jansen, E., Sinninghe Damsté, J.S.: Impact of climate change on the Baltic Sea ecosystem over the past 1,000 years. *Nat. Clim. Change* 2, 871-874, 2012.
- 880 Keeling, R. F., Garcia, H. E.: The change in oceanic O₂ inventory associated with recent global Warming. *P. Natl. Acad. Sci.* 99, 7848-7853, 2002.
- Knudsen, K.L., Jiang, H., Gibbard, P.L., Kristensen, P., Seidenkrantz, M.-S., Janczyk-Kopikowa, Z., Marks, L.: Environmental reconstructions of Eemian Stage interglacial marine records in the Lower Vistula area, southern Baltic Sea. *Boreas* 41, 209-234, 2011.



- 885 Kim, J.H., van der Meer, J., Schouten, S., Helmke, P., Willmott, V., Sangiorgi, F., Koc, N., Hopmans, E.C. Sinninghe Damsté, J.S.: New indices and calibrations derived from the distribution of crenarchaeal isoprenoid tetraether lipids: Implications for past sea surface temperature reconstructions. *Geochim. Cosmochim. Ac.* 74, 4639-4654, 2010.
- Kotilainen, A.T., Arppe, L., Dobosz, S., Jansen, E., Kabel, K., Karhu, J., Kotilainen, M.M., Kuijpers, A., Lougheed, B.C., Meier, H.E.M., Moros, M., Neumann, T., Porsche, C., Poulsen, N., Rasmussen, P., Ribeiro, S., Risebrobakken, B., Ryabchuk, D., Schimanke, S., Snowball, I., Spiridonov, M., Virtasalo, J.J., Weckström, K., Witkowski, A., Zhamoida, V.: Echoes from the Past: A Healthy Baltic Sea Requires More Effort. *Ambio* 43, 60-68, doi:10.1007/s13280-013-0477-4, 2014.
- 890 Kotthoff, U., Pross J., Müller U.C., Peyron O., Schmiedl G., Schulz H., Bordon A.: Timing and characteristics of terrestrial vegetation change in the NE Mediterranean region associated with the formation of marine Sapropel S1: A land-sea correlation. *Quaternary Sci. Rev.* 27, 832-845, 2008.
- 895 Kotthoff, U., Koutsodendris, A., Pross, J., Schmiedl, G., Bornemann, A., Kaul, C., Marino, G., Peyron, O., Schiebel, R.: Impact of late glacial cold events in the Northern Aegean region, reconstructed from integrated marine and terrestrial proxy data. *Quaternary Sci.* 26, 86-96, 2011.
- Krammer, K., Lange-Bertalot, H.: Bacillariophyceae. In: Ettl, H., Gärtner, J.G. (teil 4), Gerloff, J., Heynig, H. and Mollenhauer, D., editors, *Süßwasserflora von Mitteleuropa*, Stuttgart, New York: Gustav Fischer Verlag. 1. Teil Naviculaceae (1986). 2. Teil Bacillariaceae, Epithemiaceae, Surirellaceae (1988). 3. Teil Centrales, Fragilariaceae, Eunotiaceae (1991a). 4. Teil Achnantaceae (1991b), 1986-1991.
- 900 Kristensen, P.H., Knudsen, K.L.: Palaeoenvironments of a complete Eemian sequences at Mommark, South Denmark: foraminifera, ostracods and stable isotopes. *Boreas* 35, 349-366, 2006.
- Kristjánsdóttir, G.B., Lea, D.W., Jennings, A.E., Pak, D.K., Belanger, C.: New spatial Mg/Ca-temperature calibrations for three Arctic, benthic foraminifera and reconstruction of north Iceland shelf temperature for the past 4000 years. *Geochim., Geophys., Geosys.*, 8, Q03P21, doi:10.1029/2006GC001425, 2007.
- 905 Krossa, V.R.: Regional climate change and onset of farming in northern Germany and southern Scandinavia. The Holocene, in press. Kühl, N., Moschen, R.: A combined pollen and $\delta^{18}\text{O}_{\text{Sphagnum}}$ record of mid-Holocene climate variability from Dürres Maar (Eifel, Germany). *The Holocene* 22, 1075-1085, doi:10.1177/0959683612441838, 2012
- 910 Leppäranta, M., Myrberg, K.: *Physical oceanography of the Baltic Sea*. Springer-Verlag Berlin Heidelberg, 378 pp., 2009.
- Liu, X.L., Summons, R.E., Hinrichs, K.U.: Extending the known range of glycerol ether lipids in the environment: structural assignments based on tandem mass spectral fragmentation patterns. *Rapid Commun. Mass Sp.* 26, 2295-2302, 2012.
- Lopes dos Santos, R.A., Spooner, M.I., Barrows, T.T., De Deckker, P., Sinninghe Damsté, J.S., Schouten, S.: Comparison of organic (U^{K}_{37} , $\text{TEX}^{\text{H}}_{86}$, LDI) and faunal proxies (foraminiferal assemblages) for reconstruction of late Quaternary sea surface temperature variability from offshore southeastern Australia. *Paleoceanography* 28, 377-387, 2013.
- 915 Lutze, G.: Zur Foraminiferen-Fauna der Ostsee. *Meyniana* 15, 75-142, 1965.
- Lutze, G.: Foraminiferen der Kieler Bucht (Westliche Ostsee): 1 'Hausgartengebiet' des Sonderforschungsbereiches 95 der Universität Kiel. *Meyniana* 26, 9-22, 1974.



- Martin, P.A., Lea, D.W.: simple evaluation of cleaning procedures on fossil benthic foraminiferal Mg/Ca. *Geochem., Geophys., Geosys.* 3, 1-8, doi:10.1029/2001GC000280, 2002.
- Matthäus, W., Schinke, H.: The influence of river runoff on deep water conditions of the Baltic Sea. *Hydrobiologia* 393, 1-10, 1999.
- Mauri, A., Davis, B.A.S., Collins, P.M., Kaplan, J.O.: The Climate of Europe during the Holocene: a gridded pollen-based reconstruction and its multi-proxy evaluation. *Quaternary Sci. Rev.* 112, 109-127, 2015.
- Meier, H.E., Müller-Karulis, B., Andersson, H.C., Dieterich, C., Eilola, K., Gustafsson, B.G., Höglund, A., Hordoir, R., Kuznetsov, I., Neumann, T., Ranjbar, Z., Savchuk, O.P., Schimanke, S.: Impact of Climate Change on Ecological Quality Indicators and Biogeochemical Fluxes in the Baltic Sea: A Multi-Model Ensemble Study. *Ambio* 41:558–573, doi:10.1007/s13280-012-0320-3, 2012.
- Michalak, A.M., Anderson, E.J., Beletsky, D., Boland, S., Bosch, N.S., Bridgeman, T.B., Chaffin, J.D., Cho, K., Confesor, R., Daloğlu, I., DePinto, J.V., Evans, M.A., Fahnenstiel, G.L., He, L., Ho, J.C., Jenkins, L., Johengen, T.H., Kuo, K.C., LaPorte, E., Liu, X., McWilliams, M.R., Moore, M.R., Posselt, D.J., Richards, R.P., Scavia, D., Steiner, A.L., Verhamme, E., Wright, D.M., Zagorski, M.A.: Record-setting algal bloom in Lake Erie caused by agricultural and meteorological trends consistent with expected future conditions. *P. Natl. Acad. Sci. USA* 110 (16), 6448-6452, 2013.
- Mohrholz, V., Naumann, M., Nausch, G., Krüger, S., Gräwe, U.: Fresh oxygen for the Baltic Sea - An exceptional saline inflow after a decade of stagnation. *J. Mar. Sys.* 148, 152-166, 2015.
- Mudie, P.J., Rochon, A., Aksu, A.E., Gillespie, H.: Dinoflagellate cysts, freshwater algae and fungal spores as salinity indicators in Late Quaternary cores from Marmara and Black seas. *Mar. Geol.* 190, 203-231, 2002
- Murray, J.W.: *Ecology and Applications of Benthic Foraminifera*. Cambridge University Press, 440 pp., 2006.
- Ning, W., Anderson, P.S., Ghosh, A., Khan, M., Filipsson, H.L.: Quantitative salinity reconstructions of the Baltic Sea during the mid-Holocene. *Boreas*, doi:10.1111/bor.12156. ISSN 0300-9483, 2015.
- Ning, W., Ghosh, A., Jilbert, T., Slomp, J.P., Khan, M., Nyberg, J., Conley, D.J., Filipsson, H.L.: Evolving coastal character of a Baltic Sea inlet during the Holocene shoreline regression: impact on coastal zone hypoxia. *J. Paleolimnol.* 55, 319-338, doi:10.1007/s10933-016-9882-6, 2016.
- O'Neil, J.M., Davis, T.W., Burford, M.A., Gobler, C.J.: The rise of harmful cyanobacteria blooms: The potential roles of eutrophication and climate change. *Harmful Algae* 14, 313-334, 2012.
- Omstedt, A., Meuller, L., Nyberg, L.: Interannual, seasonal, and regional variations of precipitation and evaporation over the Baltic Sea. *Ambio* 26, 484-492, 1997.
- Osterman, L. E., Poore, R. Z., Swarzenski, P. W., Turner, R. E.: Reconstructing a 180 yr record of natural and anthropogenic induced low-oxygen conditions from Louisiana continental shelf sediments. *Geology* 33, 329-332, doi:10.1130/G21341.1, 2005.



- Passey, B. H., Levin, N.E., Cerling, T.E., Brown, F.H., Eiler, J.M., Rendle-Bürhing, R., 2010. High-temperature environments of human evolution in East Africa based on bond ordering in paleosol carbonates. *P. Natl. Acad. Sci. USA* 107, 11245-11249, 2010.
- Patrick, R. Reimer, C.W.: The Diatoms of the United States. Monographs of the Natural Academy of Sciences of Philadelphia, 955 Number 13, 688 pp, 1966.
- Platon, E., Sen Gupta, B.K., Rabalais, N.N., Turner, R.E.: Effect of seasonal hypoxia on the benthic foraminiferal community of the Louisiana inner continental shelf: The 20th century record. *Mar. Micropaleontol.* 54, 263-283, 2005.
- Raiswell, R., Canfield, D.E.: Sources of iron for pyrite formation in marine sediments. *Am. J. Sci.* 298, 219-245, 1998.
- Raitzsch, M., Kuhnert, H., Groeneveld, J., Bickert, T.: Benthic foraminifer Mg/Ca anomalies in South Atlantic core top 960 sediments and their implications for paleothermometry. *Geochem., Geophys., Geosys.* 9, Q05010, doi:10.1029/2007GC001788, 2008.
- Rampen, S.W., Willmott, V., Kim, J.-H., Uliana E., Mollenhauer, G., Schefuß E., Sinninghe Damsté, J.S., Schouten, S.: Long chain 1,13- and 1,15-diols as a potential proxy for palaeotemperature reconstruction. *Geochim. Cosmochim. Ac.* 84, 204-216, 2012.
- 965 Rampen, S.W., Datema, M., Rodrigo-Gámiz, M., Schouten, S., Reichart, G.J., Sinninghe Damsté, J.S.: Sources and proxy potential of long chain alkyl diols in lacustrine environments. *Geochim. Cosmochim. Ac.* 144, 59-71, 2014.
- Reimer, P.J., Bard, E., Bayliss, A., Beck, J.W., Blackwell, P.G., Bronk Ramsey, C., Buck, C.E., Cheng, H., Edwards, R.L., Friedrich, M., Grootes, P.M., Guilderson, T.P., Hafliðason, H., Hajdas, I., Hatté, C., Heaton, T.J., Hoffmann, D.L., Hogg, A.G., Hughen, K.A., Kaiser, K.F., Kromer, B., Manning, S.W., Niu, M., Reimer, R.W., Richards, D.A., Scott, E.M., Southon, 970 J.R., Staff, R.A., Turney, C.S.M., van der Plicht, J.: IntCal13 and Marine13 radiocarbon age calibration curves 0-50,000 years cal BP. *Radiocarbon* 55, 1869-1887, 2013.
- Rodrigo-Gámiz, M., Rampen, S.W., de Haas, H., Baas, M., Schouten, S., Sinninghe Damsté, J.S. Constraints on the applicability of the organic temperature proxies U^{K}_{37} , TEX_{86} and LDI in the subpolar region around Iceland. *Biogeosciences* 12, 6573-6590, 2015.
- 975 Rütters, H., Sass, H., Cypionka, R., Rullkötter, J.: Phospholipid analysis as a tool to study complex microbial communities in marine sediments. *J. Microbiol. Meth.* 48, 149-160, 2002.
- Schöne, B.R.: The curse of physiology—challenges and opportunities in the interpretation of geochemical data from mollusk shells. *Geo.-Mar. Lett.* 28, 269-285, doi:10.1007/s00367-008-0114-6, 2008.
- Schouten, S., Hopmans, E.C., Schefuß, E., Sinninghe Damsté, J.S.: Distributional variations in marine crenarchaeotal 980 membrane lipids: a new tool for reconstructing ancient sea water temperatures? *Earth Planet. Sc. Lett.* 204, 265-274, 2002.
- Schouten, S., Hopmans, E.C., Rosell-Melé, A., Pearson, A., Adam, P. et. al. An interlaboratory study of TEX_{86} and BIT analysis of sediments, extracts, and standard mixtures. *Geochem., Geophys., Geosys.*, 14, 1-23, 2013a.
- Schouten, S., Hopmans, E.C., Sinninghe Damsté, J.S.: The organic geochemistry of glycerol dialkyl glycerol tetraether lipids: a review. *Org. Geochem.* 54, 19-61, 2013b.



- 985 Seidenkrantz, M.-S.: Subrecent changes in the foraminiferal distribution in the Kattegat and the Skagerrak, Scandinavia: anthropogenic influence and natural causes. *Boreas* 22 (4), 383-395, 1993
- Seppä, H., Hammarlund, D., Antonsson, K.: Low-frequency and high-frequency changes in temperature and effective humidity during the Holocene in south-central Sweden: implications for atmospheric and oceanic forcings of climate. *Clim. Dynam.* 25, 285-297, 2005.
- 990 Shen, C.-C., Hastings, D.W., Lee, T., Chiu, C.-H., Lee, M.-Y., Wei, K.-Y., Edwards, R.L.: High precision glacial-interglacial benthic foraminiferal Sr/Ca records from the eastern Atlantic Ocean and Caribbean Sea. *Earth Plan. Sci. Lett.* 190, 197-209, 2001.
- Skirbekk, K., Hald, M., Marchitto, T.M., Junttila, J., Kristensen, D.K., Sørensen, S.A.: Benthic foraminiferal growth seasons implied from Mg/Ca-temperature correlations for three Arctic species. *Geochem., Geophys., Geosys.* 17, 4684-4704, doi:10.1002/2016GC006505, 2016.
- 995 Snoeijs, P. et al.: Intercalibration and distribution of diatom species in the Baltic Sea. Volumes 1-5, Vol. 1, 129 pp. (1993): Snoeijs, P. (ed.), Vol. 2, 126 pp. (1994): Snoeijs, P. & Vilbaste, S. (eds), Vol. 3, 126 pp. (1995): Snoeijs, P. & Potapova, M. (eds), Vol. 4, 126 pp. (1996): Snoeijs, P. & Kasperoviciene, J. (eds), Vol. 5, 144 pp. (1998): Snoeijs, P. & Balashova, J. (eds). Opulus Press, Uppsala, 1993-1998.
- 1000 Snoeijs, P. Weckström, K.: Diatoms and environmental change in large brackish-water ecosystems. In: Smol, J.P. and Stoermer, E.F. (eds). *The Diatoms: Applications for the Environmental and Earth Sciences*. Second edition, Cambridge University press. 287-308, 2010.
- Sohlenius, G., Sternbeck, J., Andrén, E., Westman, P.: Holocene history of the Baltic Sea as recorded in a sediment core from the Gotland Deep. *Mar. Geol.* 134, 183-201, doi:10.1016/0025-3227(96)00047-3, 1996.
- 1005 Steinke, S., Groeneveld, J., Johnstone, H., Rendle-Bürhing, R.: East Asian summer monsoon weakening after 7.5 Ma: Evidence from combined planktonic foraminifera Mg/Ca and $\delta^{18}\text{O}$ (ODP Site 1146; northern South China Sea). *Palaeogeogr. Palaeoclim.* 289, 33-43, 2010.
- Thorsen, T.A., Dale, B., Nordberg, K.: 'Blooms' of the toxic dinoflagellate *Gymnodinium catenatum* as evidence of climatic fluctuations in the late Holocene of southwestern Scandinavia. *The Holocene* 5, 435-446, 1995.
- 1010 Thorsen, T.A., Dale, B.: Dinoflagellate cysts as indicators of pollution and past climate in a Norwegian fjord. *The Holocene* 7, 433-446, 1997.
- Van Helmond, N.A.G.M., Krupinski, N.B.Q., Loughheed, B.C., Obrochta, S.P., Andrén, T., Slomp, C.P. Seasonal hypoxia was a natural feature of the coastal zone in the Little Belt, Denmark, during the past 8 ka, accepted.
- Versteegh, G.J.M., Bosch, H.J., de Leeuw, J.W.: Potential palaeoenvironmental information of C_{24} to C_{36} mid-chain diols, keto-ols and mid-chain hydroxy fatty acids; a critical review. *Org. Geochem.* 27, 1-13, 1997.
- 1015 Viehberg, F.A., Frenzel, P., Hoffmann, G.: Succession of late Pleistocene and Holocene ostracode assemblages in a transgressive environment: A study at a coastal locality of the southern Baltic Sea (Germany). *Palaeogeogr. Palaeoclim.* 264, 318-329, doi:10.1016/j.palaeo.2007.05.026, 2008.



- Visbeck, M.H., Hurrell, J.W., Polvani, L., Cullen, H.M.: The North Atlantic Oscillation: Past, present, and future. *P. Natl. Acad. Sci. USA* 98, 12876-12877, doi:10.1073/pnas.231391598, 2001.
- 1020 Volkman, J.K., Barrett, S.M., Dunstan, G.A., Jeffrey, S.W.: C₃₀-C₃₂ alkyl diols and unsaturated alcohols in microalgae of the class Eustigmatophyceae. *Org. Geochem.* 18, 131-138, 1992.
- Volkman, J.K., Barrett, S.M., Blackburn, S.I.: Eustigmatophyte microalgae are potential sources of C₂₉ sterols, C₂₂-C₂₈ *n*-alcohols and C₂₈-C₃₂ *n*-alkyl diols in freshwater environments. *Org. Geochem.* 30, 307-318, 1999.
- 1025 Warnock, J.P., Scherer, R.P.: A revised method for determining the absolute abundance of diatoms. *J. Paleolimnol.* 53, 157-163, doi:10.1007/s10933-014-9808-0, 2015.
- Wasmund, N., Uhlig, S.: Phytoplankton trends in the Baltic Sea. *ICES Journal of Marine Science.* 60, 177-186, 2003.
- Weijers, J.W.H., Schouten, S., Spaargaren, O.C., Sinninghe Damsté, J.S.: Occurrence and distribution of tetraether membrane lipids in soils: implications for the use of the TEX₈₆ proxy and BIT index. *Org. Geochem.* 37, 1680-1693, 2006.
- 1030 Willumsen, P.S., Filipsson, H.L., Reinholdsson, M., Lenz, C.: Surface salinity and nutrient variations during the Littorina Stage in the Fårö Deep, Baltic Sea. *Boreas* 42, 210-223, doi:10.1111/j.1502-3885.2012.00286x, 2013.
- Yu, S.-Y., Berglund, B.-E.: A dinoflagellate cyst record of Holocene climate and hydrological changes along the southeastern Swedish Baltic coast. *Quaternary Res.* 67, 215-224, 2007.
- Zhu, C., Weijers, J.W.H., Wagner, T., Pan, J.M., Chen, J.F., Pancost, R.D.: Sources and distributions of tetraether lipids in surface sediments across a large river-dominated continental margin. *Org. Geochem.* 42, 376-386, 2011.
- 1035 Zillén, L., Conley, D.J., Andren, T., Andren, E., Björck, S.: Past occurrences of hypoxia in the Baltic Sea and the role of climate variability, environmental change and human impact. *Earth Science Reviews*, 91, 77-92, doi: 10.1016/j.earscirev.2008.10.001, 2008.
- Zink, K.G., Vandergoes, M.J., Bauersachs, T., Newnham, R.M., Rees, A.B.H., Schwark, L.: A refined paleotemperature calibration for New Zealand limnic environments using differentiation of branched glycerol dialkyl glycerol tetraether (brGDGT) sources. *J. Quat. Sci.* 31, 823-835, 2016.
- 1040 Zonneveld, K.A.F., Pospelova V.: A determination key for modern dinoflagellate cysts. *Palynology* 39 (3), 387- 409, doi: 10.1080/01916122.2014.990115, 2015.



1045 **Figure 1: Map of the southern Baltic Sea (redrawn from Groeneweld and Filipsson, 2013). The positions of Integrated Ocean Drilling Program Site M0059 (white star; 55°0.29'N29'N, 10°6.49'E49'E; Andrén et al., 2015a) and of Lake Belau in northern Germany (black point; Dörfler et al., 2012) are indicated. Continuous (surface) and dashed (bottom) lines indicate dominant current directions.**

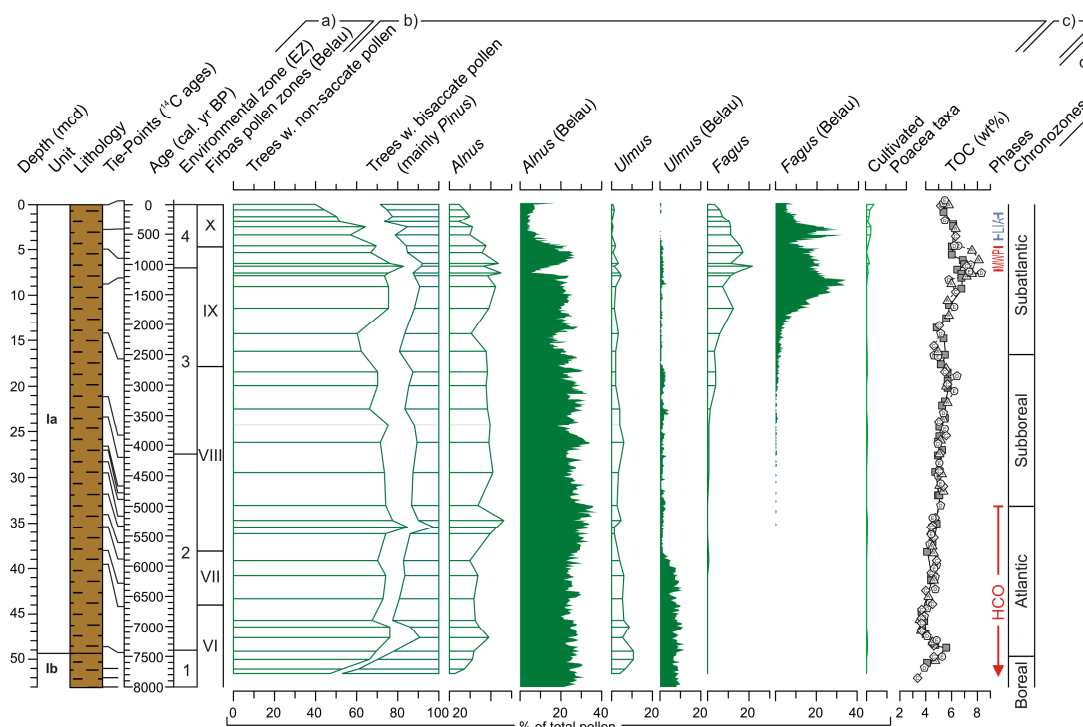
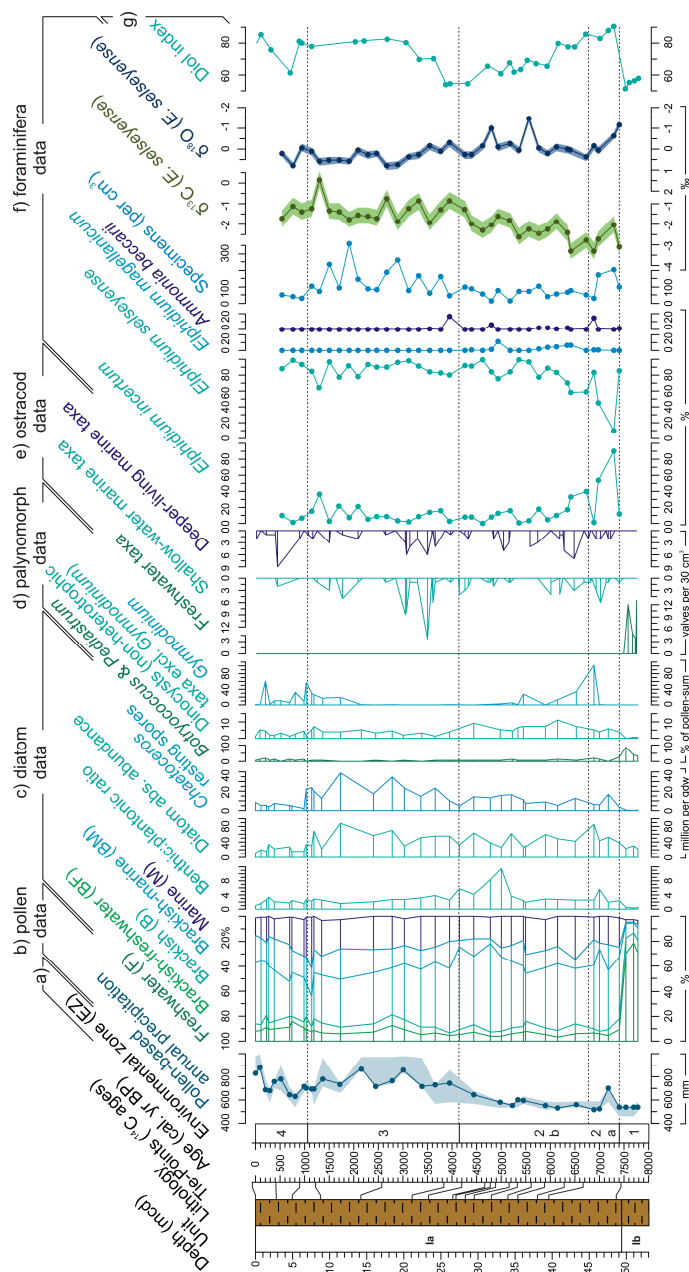


Figure 2: Comparison of the pollen record from Site M0059 with the varved pollen record of Lake Belau (northern Germany, Dörfler et al. 2012). Sedimentological units, lithology (Andrén et al., 2015a), position of ^{14}C ages (Van Helmond et al., accepted) plotted vs. depth; plotted vs. age (extrapolated below ~48.64 mcd): a) environmental zones (EZ; Site M0059), Firbas pollen zones (Lake Belau), b) selected pollen taxa (w. horizontal bars: M0059, filled: Lake Belau), c) total organic carbon (TOC; white: shipboard data – triangles: Hole A, rhombi: Hole C, pentagons: Hole D, circles: Hole E; grey squares: onshore data) for Site M0059, d) climate phases and chronozones.

Figure 3 (next page): Sedimentological units, lithology (Andrén et al., 2015a), position of ^{14}C ages (Van Helmond et al., accepted) vs. depth; M0059 precipitation and salinity proxies plotted versus age (extrapolated below ~48.64 mcd): a) environmental zones (EZs) based on diatom data; b) pollen-based precipitation reconstructions based on the modern analogues technique; c) diatom salinity-based affinities and life forms (benthic vs. pelagic) following Snoeijs et al. (1993-1998); d) palynomorphs/pollen ratios based on total amount of terrestrial pollen, freshwater algae comprising *Botryococcus* and *Pediastrum* species, dinocysts predominately comprising cysts of *Protoceratium reticulatum* (*Operculodinium* cysts), *Lingulodinium*, and *Spiniferites* species (*Gymnodinium* excluded); e) Ostracod shallow water/deeper living marine taxa plotted from right to left; f) total abundance of benthic foraminifera per cm^3 of dried sediment with the relative abundance of the most common species; benthic foraminiferal taxa (*Elphidium incertum*, *E. selseyense*, *E. magellanicum*, and *Ammonia beccarii*) shown as % of total benthic foraminiferal fauna; total abundance of benthic foraminifera shown as specimens per cm^3 of dried sediment; stable carbon and oxygen isotope data analysed on *E. selseyense*; f) Diol Index (DI) indicating relative changes in surface water salinity.



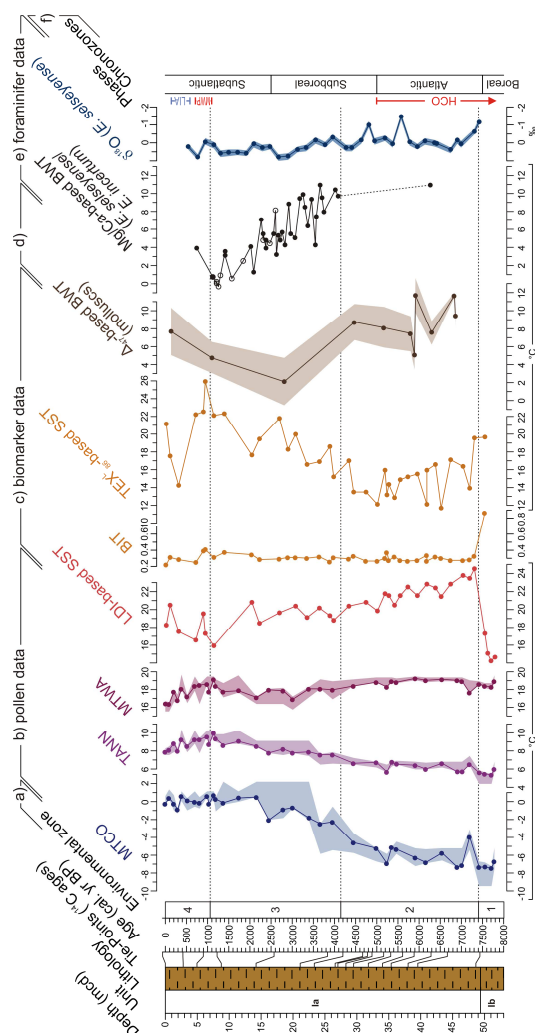


Figure 4: Sedimentological units, lithology (Andr n et al., 2015a), position of ^{14}C ages (Van Helmond et al., in review) vs. depth; M0059 temperature proxies plotted versus age (extrapolated below ~48.64 mcd): a) environmental zones (EZs) based on diatom data; b) pollen-based climate reconstructions based on the modern analogues technique, shaded area reflects the range of the best 10 analogues; c) LDI and TEX^{1-86} reflecting summer SSTs; BIT shown as quantitative measure for the amount of terrestrial organic matter transported to marine realm; d) $\Delta 47$ -inferred temperatures based on clumped isotope composition of mollusc material; e) Mg/Ca-based BWT using the benthic foraminifera *E. selseyense* and *E. incertum*; stable oxygen isotopes based on the benthic foraminifera *E. selseyense*; f) climate phases and chronozones. MTCO = mean temperature coldest month, TANN = annual temperature, MTWA = mean temperature warmest month, SST = surface water temperature, BWT = bottom water temperature.

1075